Environmental Modelling and Software 126 (2020) 104641

Contents lists available at ScienceDirect

Environmental Modelling and Software

journal homepage: http://www.elsevier.com/locate/envsoft

Exploring reciprocal interactions between groundwater and land cover decisions in flat agricultural areas and variable climate

Moira Zellner [a,*], Guillermo A. García [b,c], Federico Bert [c], Dean Massey [a], Marcelo Nosetto [b,d]

[a] The University of Illinois at Chicago, United States
[b] Grupo de Estudios Ambientales, Instituto de Matemática Aplicada San Luis (IMASL), CONICET and Universidad Nacional de San Luis, Argentina
[c] CREA Argentina, Argentina
[d] Cátedra de Climatología Agrícola, Facultad de Ciencias Agropecuarias, Universidad Nacional de Entre Ríos, Argentina

ARTICLE INFO

Keywords:
Natural-human systems modeling
Rural decision-making
Water table
Water risk management
Pampas

ABSTRACT

We present Hydroman, a flexible spatially explicit model coupling human and hydrological processes to explore shallow water tables and land cover interactions in flat agricultural landscapes, modeled after the Argentine Pampas. With fewer parameters, Hydroman aligned well with established hydrological models, and was validated with observed water table patterns and crop yield data. Simulations with different climate, phreatic and land cover conditions confirmed that climate remains the main driver, but crops also influence water levels and yields, depending on the growing cycle. We also examined the impacts of two alternative sowing strategies. Risk aversion proves robust in minimizing crop losses, but often results in less sowing, exacerbating flooding. Strict rotators risk more, but help stabilize the groundwater levels. Reintroducing pasture further stabilizes the system. Future work will engage farmers to derive and assess land cover strategies that maximize yield and minimize losses, and transfer our modeling approach to other applications.

1. Introduction

In rainfed agricultural systems, groundwater affects agricultural productivity and, ultimately, farmers' land cover decisions. If the water table is too deep, groundwater cannot be reached by crop roots, so that crop growth depends mostly on rainfall. Crops yields grow exponentially as the water table approaches the root zone, enabling capillary water supply from the saturated zone (Kang et al., 2001; Nosetto et al., 2009). When the water table lies at this optimum depth, groundwater can supply most of the crop's water requirements, mainly in dry years. However, crop yields fall sharply as water table levels continue to increase, creating saturated conditions within the crops' root zone (Mueller et al., 2005; Nosetto et al., 2009).

Flat landscapes with humid climates, like the Argentine Pampas, the Carpathian basin or the Great Plains of western Canada, are particularly vulnerable to flooding because the water table tends to oscillate close to the soil surface (Fan et al., 2013; Jobbágy and Jackson, 2004). As a consequence, these areas may be waterlogged for prolonged periods, not only reducing crop yields but also affecting available land, machinery use and transport logistics (Aragón et al., 2011; Viglizzo et al., 2009). In such landscapes, regional horizontal water flows are relatively limited, also due to low soil hydraulic conductivity, while vertical water inputs and outputs dominate the water balance (Mercau et al., 2016). Thus, groundwater levels in flat landscapes mainly follow rainfall variability (Portela et al., 2009) and the main water outputs are plant consumption and soil evaporation, which are in turn influenced by land cover decisions (Nosetto et al., 2012).

The magnitude and timing of evapotranspiration together with root depth and waterlogging tolerance vary among crops. For instance, pastures, which grow during the whole year and have a deeper root system, may consume almost twice the water used by annual cash crops like soybean, which occupy the field only part of the year (4–5 months) (Nosetto et al., 2009, 2015). Farmers' agronomical practices may also affect groundwater dynamics, like no-tillage cropping that leave the soil undisturbed and covered with stubble to reduce soil evaporation (Sinclair et al., 2007). In other words, farmers' decisions introduce a reciprocal relationship with water table dynamics, and they are both influenced by climate variability.

The effects of land cover on groundwater could encourage farmers to make cropping decisions to keep the water table level in the "sweet zone" (Nosetto et al., 2012), i.e., between 1.5 and 2.5 m from the soil surface (Nosetto et al., 2009). Achieving this is not straightforward,

* Corresponding author.
E-mail address: mzellner@uic.edu (M. Zellner).

https://doi.org/10.1016/j.envsoft.2020.104641
Received 27 July 2019; Received in revised form 20 January 2020; Accepted 22 January 2020
Available online 29 January 2020

however. First, farmers make land cover decisions within their plots, while water flows through property lines. Heterogeneous land covers across a landscape may trigger horizontal groundwater flows, introducing interdependency among farmers sharing the same phreatic aquifer (García et al., 2017). Therefore, water table depth at the farm level depends not only on the farmer's land cover decisions, but also on the decisions of the neighboring farmers. Second, the amount of rain during the cropping cycle (one of the main drivers of groundwater dynamics) is highly uncertain and variable, which translates into greater uncertainty for farmers regarding the impacts of their land cover decisions (Mercau et al., 2016).

Understanding linkages between climate variability, groundwater dynamics and land cover decisions is central to the sustainability of coupled water and agriculture systems. Water for food production exceeds all other water needs, and water also drives several important ecosystem functions. The proposal of managing water table depth to enhance the sustainability of water and agriculture should be based on a deep understanding and assessment of these linkages, from the individual farm level through the landscape level (Gleeson et al., 2012; Rosegrant et al., 2009; Wada et al., 2010).

Existing models are difficult to use for this purpose; they tend to be either too simple or too complicated, which makes them unsuitable to test a wide range of scenarios and include the explicit representation of decision-making. GUARDA is an example of a simple spreadsheet-based model used to make site-specific estimates of agricultural soil water content (Mercau and Jobbágy (2013). In its current form, it does not allow for the representation of the spatial context and cross-scale interactions. On the other extreme, detailed process-based and spatially explicit models are data intensive and are costly to calibrate and parameterize. MIKE SHE was created to provide a wide range of customizable water mass balance outputs for nearly all types of hydrology (Refsgaard and Storm, 1995; Refsgaard et al., 2010). Given its underlying computational complexity, the number of time steps is limited to 800, calibration is extensive, and recommended resolution is low, to ensure that simulations can be completed within reasonable time frames. Hydrus was developed to analyze movements of water, heat, and solutes in porous media and is available in versions that are either two- or three-dimensional (Šimůnek et al., 2005). Time steps may be as small as 1 s, which, together with a hexahedral geometry, yields higher precision results. Precision comes at the expense of flexibility in scenario testing and parameterization, however, which limits its applicability and slows downs simulations. While originally developed to model groundwater flow, MODFLOW now includes several modules that simulate additional processes (Langevin et al., 2018). MODFLOW is a data intensive numerical model, but the modularity of the model can make it easier to run faster simulations than with other process-based models if fewer outputs are desired. Surface water flows are harder to simulate in MODFLOW, however. DRAINMOD-DSSAT seeks to optimize drainage in agricultural soils, assuming surface and sub-surface drainage infrastructure and not lateral groundwater flow (Skaggs 1978; Negm et al., 2014). Outputs include water mass balance data and crop yields. This model was not intended for conditions other than humid climates, slight slopes, and the presence of drainage networks, however.

While the above models are extensively used, they do not explicitly consider the human dimension. Although some cases exist of coupling these sophisticated hydrological models to human decision-making (e.g., García et al., 2019; Reeves and Zellner, 2010; Zellner and Reeves, 2010), these efforts take considerable amount of time and funding to both develop and run. Our aim was to develop a simpler and more agile spatially explicit platform that recreates enough of both the hydrological and social complexity of flatland agricultural systems to rapidly explore the effects of a wide range of climate and decision-making scenarios (Castilla-Rho et al., 2015; Zellner, 2007). Such a platform would also be more useful to stakeholders and decision-makers to explore the unintended consequences of their individual and collective decisions.

This paper has two main objectives. First, we describe our model, which we called Hydroman (HYDROlogy + huMAN), and validate it against other established hydrological models and field data to assess its capability to reproduce primary patterns in hydrological processes. Second, we introduce land cover decision-making processes to understand and assess interactions between climate, land cover and groundwater dynamics in agricultural systems of the Argentine Pampas. The last section builds on this understanding to explore joint land and water management implications.

1.1. Case study

Our work targets the area of the Salado A Basin, a part of the Río de la Plata hydrographic system, and specifically a site in Pehuajo (Fig. 1). This Salado basin is in the Argentine Pampas, a key agricultural area for global food security (Calviño and Monzon, 2009; Hall et al., 1992). The Pampas is one of the flattest areas in the world, with regional slopes of less than 0.1% (Jobbágy et al., 2008), and also show a strong climate variability on inter-annual (Goddard et al., 2001) to inter-decadal scales (Boulanger et al., 2005; Rusticucci and Penalba, 2000). As a result of its flat topography and significant climate variability, floods and droughts have been reported in the Salado Basin since colonial times.

Given that the majority of agricultural production in the Salado A Basin is rainfed, productivity of annual crops is strongly affected by rainfall and water table variations (Nosetto et al., 2009; Podestá et al., 1999). Since the 1970s, the Pampas showed a steady increase in late spring and summer rains, particularly near the western boundaries (Berbery et al., 2006). In the same period, there was a transition from grasslands and pastures to annual grain crops, mainly soybean (Paruelo et al., 2005; Viglizzo et al., 2011). This land cover change emerged from individual farmers' land cover decisions (Bert et al., 2014). As result of higher precipitations and a dominance of annual crops that consume less

Fig. 1. Salado A Basin (target area), highlighting the Pehuajó site for model calibration and validation.

water than perennial pastures and grasslands, water table levels have risen (Nosetto et al., 2015; Viglizzo et al., 2009).

Much uncertainty remains regarding the projected paths of future climate, land cover, and technological change in the Pampas, and there is growing concern among farmers and policy makers about potential effects on groundwater levels, particularly on the risk of flooding. In the Salado A Basin in particular, there is an increasing need to understand how management practices can help prevent flooding while maintaining water table at depths that reduce the impacts of droughts (García et al., 2019). We developed Hydroman to understand and provide insights regarding these questions, in the hope that this may be relevant to similar agricultural regions in the world.

2. Model components and processes

2.1. Model overview

Hydroman simulates the main hydrological processes relevant to our questions: land cover decisions, precipitation, evapotranspiration, and both surface and subsurface water flow. The model tracks the water contents and depths in the soil horizons (groundwater, capillary, upper, and root zones) as well as on the surface. Further, the model also keeps track of crop yields, as they are affected by water availability. In contrast to other models, each 40-year run takes 2–3 min in a 2.8 GHz processor laptop.

2.2. Landscape

The landscape is represented as a square grid, with the size of lattice determined by the user, depending on the scenario chosen. In all of the experiments completed for this publication, the size of each cell was 1 ha (100 m × 100 m) but the size can be adjusted by the user. Boundary conditions can be set to be open, where cells at the edge of the domain maintain a constant groundwater head during groundwater flow, or can be set to be closed, assuming that the landscape acts as a self-contained basin and no water can flow in or out through the edges. While this choice is left to the user to adapt boundary conditions to specific landscape representation (size and resolution), this must be thoroughly tested to understand how edge effects may influence results.

2.2.1. Land cover

Each cell of the simulated landscape can have one of seven different land cover options throughout a year: pasture, maize, a cover crop of minimal economic value, wheat, regular soybean, short-cycle soybean, and fallow (no crop). Sowing decisions during a simulation determine the land cover at any point during a year for each cell (Section 2.3.4). In some scenarios, the land cover may change during a year or between years (Section 4.2). Each land cover type has unique daily values for water need for transpiration (K_{cb}, the basal crop coefficient[1]) and rooting depth and critical growing periods when partial unmet water need directly affects yields (Fig. 2). Both K_{cb} and root depth dynamics were built based on crop simulations carried out with DSSAT (Decision Support System for Agrotechnology Transfer) models (Jones et al., 2003), literature values (Allen et al., 1998; Satorre et al., 2003) and expert knowledge. The critical growth periods for soybean, maize, and wheat yields are linked to a short period of high-water demand, a window of time spanning 30 days before and after the day with the maximum K_{cb} during a cycle. In contrast, pasture and cover crops are assumed to have critical demand for water every day they are alive (they produce biomass, rather than a commercial product), meaning that unmet water demand for the entire crop cycle affects their yields. Soybean, maize, wheat and cover crops were assumed to be able to tolerate only seven consecutive days (it can be adjusted by the user between 0 and 10 days) without any water before dying, whereas pasture is more resilient and will never fully die once sown (Sheaffer et al., 1988).

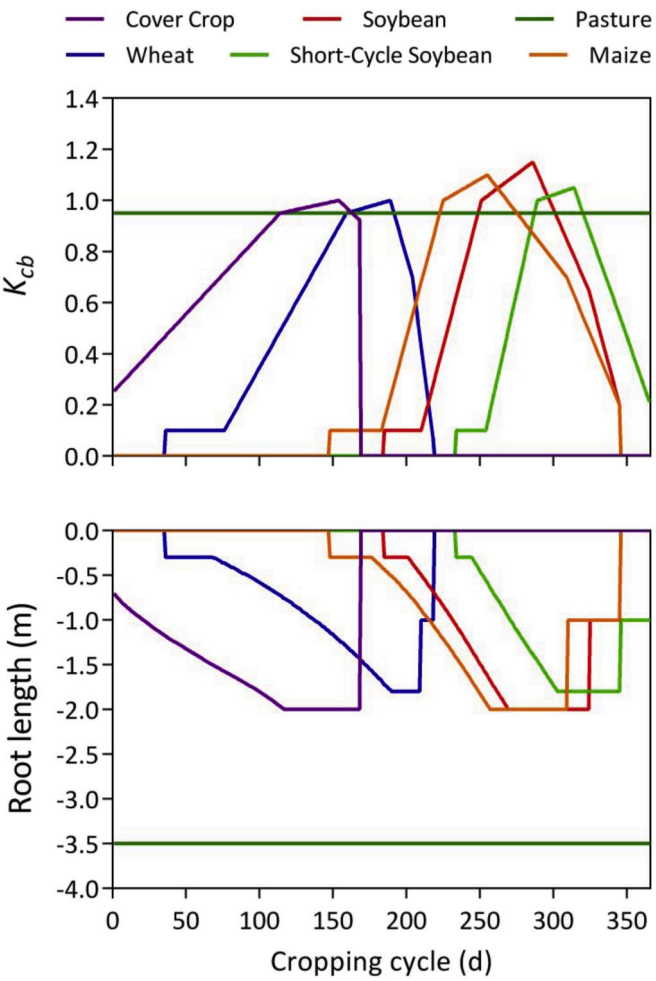

Fig. 2. Basal crop coefficient (K_{cb}) and root length dynamics used as input data by Hydroman for each land cover option. Dates defined as start - end (i.e., harvest) of grow cycle are: May 1st - October 15th for cover, June 5th - December 4th for wheat, September 25th - April 10th for maize, November 1st - April 30th for soybean, and December 20th - April 30th for short-cycle soybean. Days of maximum K_{cb} are October 1st for cover, November 5th for wheat, January 10th for maize, February 10th for soybean, and March 9th for short soybean. Pasture grow cycle occurs during the whole simulated period, keeping the K_{cb} constant.

2.2.2. Elevation and slope

Given the little variation in ground elevation, characteristic of the Argentine Pampas, slopes can be set with a slider, or an import file with values for each cell. The former option produces a stylized landscape that is useful for model verification, but the latter option can apply elevations from digital elevation models, which is useful for model validation and scenario testing. Elevation is in absolute meters above sea level.

2.2.3. Soil horizons

The soil reaches a total depth of −100 m in all cells. Soil is divided into four separate zones, as described in the following sections (Fig. 3), and is assumed to have three pore sizes: small, medium and large. The

[1] The basal crop coefficient (K_{cb}) is defined as the ratio of the crop evapotranspiration over the reference evapotranspiration (ET_c/ET_o). For more details see Allen, R.G., Pereira, L.S., Raes, D., Smith, M., 1998. Crop Evapotranspiration: guidelines for computing crop water requirements. FAO Irrigation and Drainage Paper No. 56. FAO, Rome, Italy.

small pores are assumed to be always saturated, but their water is unavailable for flow or evapotranspiration due to surface tension (matrix potential). The large, free-draining pores are assumed to be always empty because of gravitational force, unless located in the groundwater zone, where they are saturated. Medium pores can show different degrees of saturation due to infiltration, evapotranspiration, or water transfers between horizons due to changes in the groundwater levels. The proportion of small, medium and large pores in the soil is set by the user. In all of the experiments completed for this publication, medium and large pores occupied 12% and 19% of soil volume, respectively, which would correspond to the typical sandy loam soil of the region. The soil horizons are dynamic and their depths change as roots grow and groundwater flows horizontally and vertically.

Groundwater zone: The groundwater zone makes up the deepest and largest portion of the soil column. Both the large and medium pores are fully saturated and water can flow horizontally between cells if there are differences in hydraulic heads (Section 2.3.3). Soil in this zone is devoid of oxygen, so any portion of plant roots that reach into this zone will die.

Capillary zone: For the typical soil type of the study region (i.e., sandy loam Mollisol), this was set as the 0.8 m above the top of the groundwater zone. Its medium pores remain fully saturated, due to capillary action that draws water from the groundwater zone. Plants can safely draw water from this zone.

Root zone: This is the top horizon. The root zone is any part of the soil column above the capillary zone into which the plant's roots grow. At a minimum, the root zone is assumed to be 0.3 m in depth, limited by available soil column above the capillary zone, whether roots occupy that space or not, to represent the greater influence of evaporation close to the soil surface. Plants can draw water from the medium pores in the root zone for transpiration.

Upper zone: This is any soil column between the capillary and root zones, to account for water that may be stored in the soil. This water will be available for transpiration as the root grows and expands the root zone into the upper zone, or will add to the groundwater as the water table rises into the upper zone.

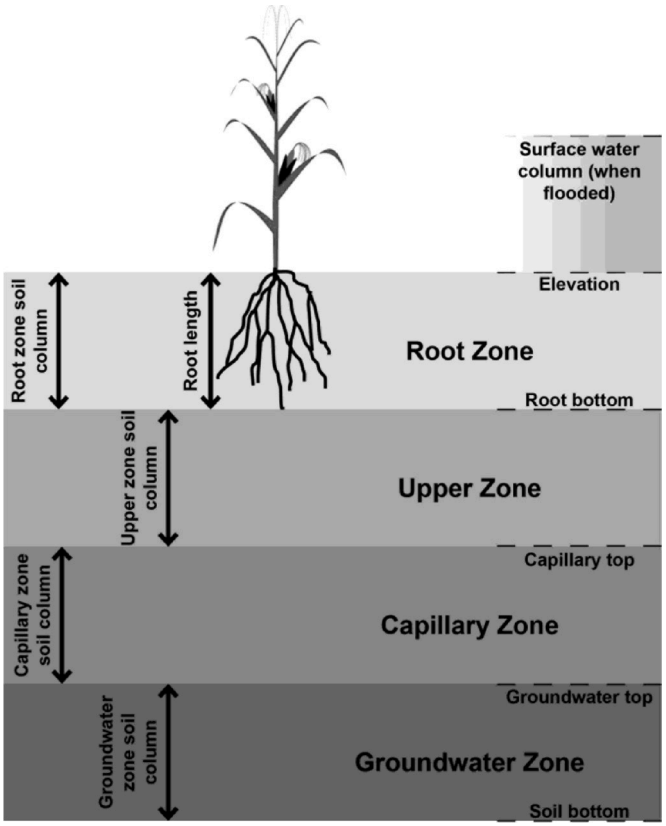

Fig. 3. Soil horizons represented in Hydroman.

2.3. Processes and order of events

Hydroman represents daily cropping and hydrological processes that are most relevant to our research questions. The processes run in the following order (Fig. 4): (1) precipitation, runoff, and infiltration, (2) surface flow, (3) groundwater flow (4) sowing decisions, (5) plant growth, (6) evapotranspiration, and (7) harvesting. Additionally, soil horizons adjust after every change in hydraulic head or root length in any of these processes.

2.3.1. Precipitation, runoff, and infiltration

The model uses daily precipitation amounts from input files that can represent either hypothetical or observed data over a number of years. Each day, the model reads the daily precipitation from the file and this value is applied to each cell as follows. Hydroman assumes a fixed percentage (which can be set by the user) of the amount will be runoff, and the rest immediately infiltrates where it falls. In all of the experiments completed for this publication, runoff was set at 30%, a reasonable value for this type of soil (Mercau, pers. comm.). The rain that infiltrates first fills unsaturated volume in the medium pores of the root zone. If there is not enough room in the root zone for all the water, the remaining rainwater fills up the medium pores of the upper zone. Any further remaining water is added to the groundwater zone, since the medium pores of the capillary zone are by definition already saturated. In this case, the groundwater level rises by an amount that depends on the amount of water transferred and the specific yield of the soil. If there is not enough room in the medium or large pores in the soil for water that is infiltrating, then the water that cannot infiltrate stays on the surface, and is added to the fixed runoff amount. The soil horizons are adjusted to reflect the change in the groundwater table (Section 2.3.8).

2.3.2. Surface flow

Each iteration, water flows from a high hydraulic head to a low hydraulic head. To do this, cells are sorted in ascending order of elevation, and sequentially interact with each one of its upstream neighbors to exchange water, also in ascending order of elevation. During the interaction, the cell determines the difference in hydraulic heads between itself and the neighbor with which it is interacting. Then, this difference in hydraulic head is divided in half, to estimate the water flow between the cell and its neighbor needed to reach equilibrium. If the neighbor's head is higher, water flows into the cell, constrained by the amount of the neighbor's water. If the reverse is true, water flows out to the neighbor, constrained by the amount of water in the originating cell. This setup results in asynchronous updating of water levels, where each pair of cells is updated one at a time, rather than all simultaneously. Since iterations are one day in length and surface water under normal conditions can be expected to reach an equilibrium level by the end of a day, this removes the need for a more intensive surface flow algorithm that accounts for factors including surface roughness, velocity, or routing.

2.3.3. Groundwater flow

The process for groundwater flow in this model builds on a previous implementation of Darcy's law of flow (Zellner, 2007; Zellner et al., 2012). Each time step, cells asynchronously exchange water with each of their neighbors. First, the flow volume is calculated according to Equation (1):

$$Q = K \times e_l \times D \times \Delta h \quad (1)$$

Where:

Q = volume of flow in m^3 per day

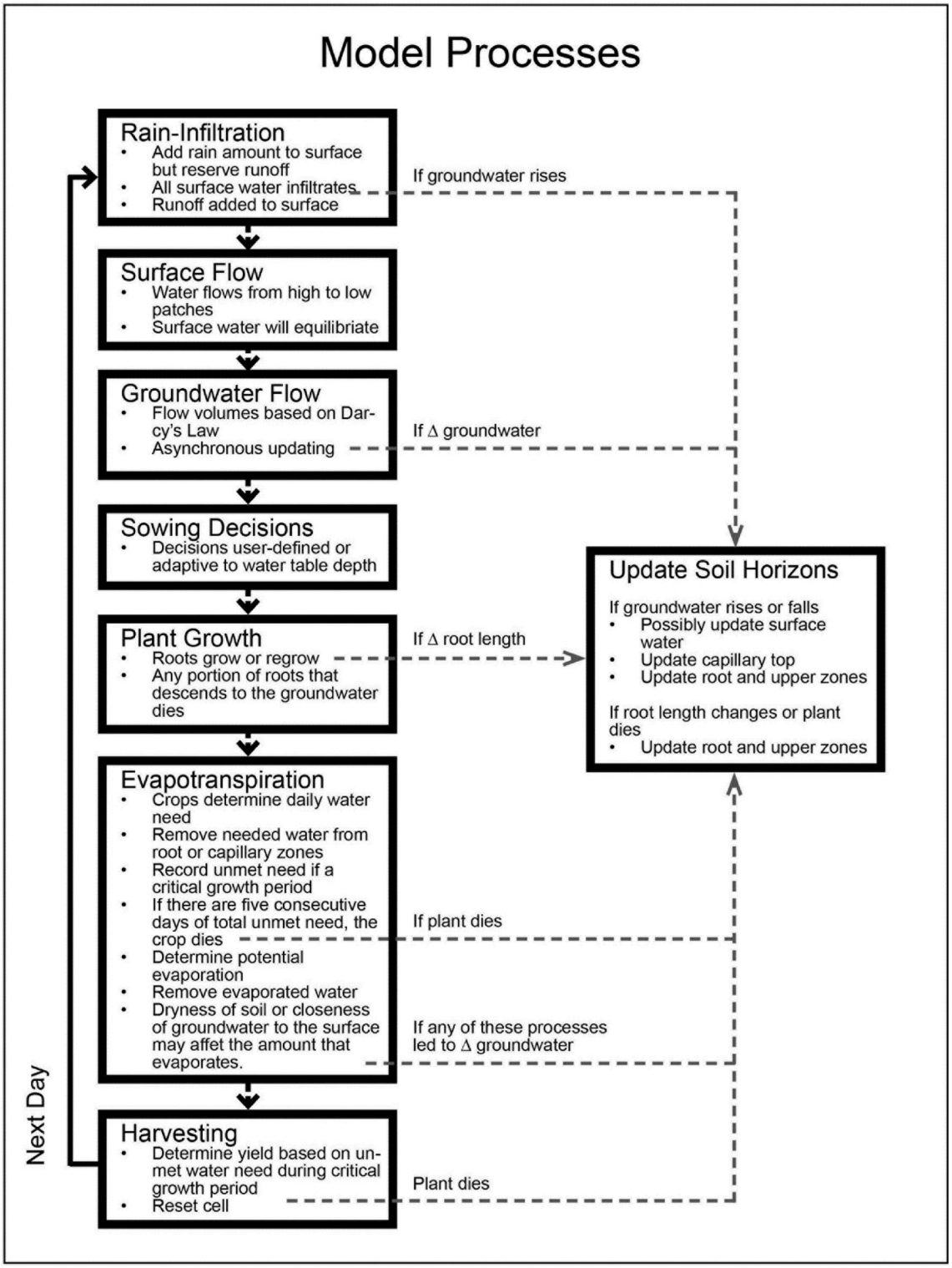

Fig. 4. Processes represented by Hydroman and order of events in a given simulation.

K = hydraulic conductivity per day
e_l = large pore specific yield (i.e., % porosity)
D = aquifer depth in the cell in m
Δh = difference in hydraulic heads between the cell and its neighbor in m

The water is transferred and cells update their water table depths based on the content of water added or subtracted. If the top of the groundwater zone is at the surface, the height of the surface water column is added to the hydraulic head to calculate flow and transfer. After all cells have finished transferring water, the model adjusts the soil horizons of the zones that are above the groundwater (including surface water if the water table reaches the surface), for the cells whose groundwater level changed (Section 2.3.8).

2.3.4. Sowing decisions

Sowing decisions are determined exogenously by the user, and are taken at the start of a new cropping cycle (May 1, or day 0). Unless the crop begins growth on the first day (pasture or cover), crops are sown seven days before its K_{cb} is first greater than 0, which happens when the plant starts growing and transpiring. When sowing happens, root growth, root damage by flooding, and yield variables for the cell are reset. Pasture does not reset root damage because it is assumed that it never truly dies or gets sown anew; it is a perennial crop, while the over crops are annual.

After an initial set of sensitivity tests (Section 3), we modified the model to include adaptive (risk-averse) farming strategies, determined endogenously based on the water table depth at different times during the cycle, and the crop rotation schedule. These will be explained in more detail in Section 4.2.

2.3.5. Plant growth

Every crop has unique daily root lengths corresponding to the time in its cropping cycle, as determined by the input file (Fig. 2). Each day, a first check for prior root damage due to contact with the water table is performed in cells with live crops (i.e., not yet harvested and with positive water demand for transpiration). If undamaged, the root length of each cell is updated according to the input file. If by doing so the roots enter the groundwater zone, the root length only grows up to the water table depth (the part of the root within the groundwater zone dies due to hypoxia) and is marked as damaged. If the roots were previously damaged, they may grow back depending on the crop type and available space above the water table. For all crops except pasture, damaged roots regrow the amount corresponding to the growth for that day. Since pasture's root length is held constant throughout the year, they are set to regrow 1% of the root length when they are damaged up to the length of an undamaged root. The cells will later use the new root lengths to update their root and upper zones (Section 2.3.8).

2.3.6. Evapotranspiration

Soil evaporation and crop transpiration are directly linked to daily reference evapotranspiration (ET_o). Potential crop evapotranspiration (ET_c) is a function of the crop's demand for water (i.e., K_{cb}) and ET_o (Equation (2)), and soil evaporation E is simply the difference between ET_o and T for the crop (Equation (3)). This means that on a given day, if T is high (when the crop is at a critical stage and leaf coverage is maximized), then E will be low because the soil will be shaded by the foliage (Allen et al., 1998).

$$ET_c = ET_0 \times K_{cbi} \tag{2}$$

Where:

ET_c = potential evapotranspiration (i.e., the daily water needs) for crop i, in m per unit area
ET_0 = daily reference evapotranspiration in m per unit area
K_{cbi} = the basal coefficient for crop i

$$E_i = ET_0 - T_i \tag{3}$$

Where:

E_i = daily soil evaporation in m per unit area
ET_0 = daily reference evapotranspiration in m per unit area
T_i = transpiration for crop i in meters per unit area

First, the model computes the daily water need for each crop type (Equation (2)). Daily water need (i.e., ET_c) for each cell is updated based on its cover, or set to zero when fallow. The soil zone from which water will be drawn for transpiration is determined by considering the proportion of roots located in the root and capillary zones. Then the actual amount of water that is available is computed, assuming that at most 10% of water that is reachable is available for transpiration at each time step (Dardanelli et al., 1997).

Next, plants are allowed to draw water from the two zones sequentially, starting with the root zone, and corresponding to the shares as computed above. If after withdrawing water from the root zone there is still unmet need, and any of its roots are in the capillary zone, then the plant will continue to withdraw any unmet need from the capillary zone. Any deficit in daily water need (i.e., whatever need remains unmet) is recorded (Equation (4), taking a value between 0 and 1, where 0 is completely met and 1 is completely unmet water need), and the cumulative percent unmet demand for the critical growth period in the current growing cycle is calculated and then averaged over the critical period. A counter keeps track of the number of consecutive days in which no water has been withdrawn by the crop. If the counter reaches 7 consecutive days and the crop is anything except pasture, the plant dies, the root length is set to 0 and both root and upper zones adjust accordingly (Section 2.3.8). Finally, the total daily transpiration amount from both zones is recorded.

$$UW_i = \frac{TWD_{CGPi}}{TWN_{CGPi}} \tag{4}$$

Where:

UW_i = daily unmet water need for crop i *(0–1)*
TWD_{CGP} = daily water deficit during the critical growth period for crop i
TWN_{CGP} = daily water need during the critical growth period for crop i

The cell's daily potential soil evaporation (E_i) is now determined (Equation (3)). When groundwater is at the ground surface, E_i is increased by 20%, due to water being more readily available to evaporate from either the surface or the groundwater itself. If there is surface water, the E_i amount is first subtracted from the surface water column. If there is still remaining E_i after all surface water evaporates, the evaporating water will be withdrawn from the groundwater at the same increased rate. If the capillary zone is at the surface, then E_i will be subtracted from the groundwater, but at the base rate. In the case where neither groundwater or capillary zones are at the surface, evaporating water will be withdrawn from the root zone (the upper zone by definition will always be too far from the surface for water to evaporate from it). In this situation, the amount of water that will evaporate from this zone depends on the saturation of its medium pores (Equation (5)).

$$E_r = E_i \times \theta \tag{5}$$

Where:

E_r = root zone evaporation amount in height (m) per unit area
E_i = potential daily soil evaporation in m
θ = the soil water content of the medium pores in the root zone (%)

Evaporation only takes water from the first 0.2 m of soil because it is assumed that below this depth direct evaporation is negligible (Jalota and Prihar, 1990; Schwartz et al., 2010). If the root zone's height is less than 0.2 m because the water table is close to the surface, any amount of E_i not withdrawn from the root zone is removed from the groundwater. After the evapotranspiration process, if the groundwater zone shrank due to evaporation or transpiration, soil horizons are updated (Section 2.3.8).

2.3.7. Harvesting

There are critical growth periods, when the amount of water consumed has a direct relationship on the crop yield at harvest (Calviño and Sadras, 2002; Calviño et al., 2003). During the critical growth period, the unmet water needs are recorded (Equation (4)). At harvest

day, i.e., the last day that a crop's K_{cb} is greater than 0, a crop yield factor is calculated for each cell based on the average water deficit during the critical period. If the plant died before harvest, then the unmet demand is assumed to be 100% for that year, which will mean there is no yield. Cumulative unmet daily need and days the length the crop was in critical growth are then reset.

The model then translates the crop yield factor into crop production, based on the potential yield for an area the size of the cell (Equation (6)). Since harvest results in plant death, the root length is set to 0 at that time, which may result in an updating of the horizons for the root and upper zones.

$$Y_i = (1 - F_Y) \times PY_i \quad (6)$$

Where:

Y_i = the annual yield for crop i on this cell, in metric tons.
F_Y = crop yield factor.
PY_i = the potential yield, or maximum annual tonnage possible for crop i on an area the size of this cell. This is the yield when $F_y = 0$. PY_i is defined by users. In all of the experiments completed for this publication, PY_i was 5, 6, 14, 5.5, 3.5 and 8 Tn ha^{-1} for cover, wheat, maize, soybean, short soybean and pasture, respectively.

2.3.8. Updating horizons

Soil horizons are updated whenever there is a change in groundwater levels, or root lengths.

Groundwater rises: Groundwater levels can rise only due to infiltration or groundwater flow. When this happens, the capillary, root, and upper zones need to be adjusted. The new sizing of the zones follows the rules outlined in Section 2.2.3. Soil that was previously in upper or even root zones may now be in the groundwater or capillary zones. Thus, the amount of water in the upper and root zones will decrease if the size of the zones decrease, but the overall % saturation of the medium pores in the root and upper zones will remain unchanged.

Groundwater falls: Groundwater levels can fall only due to groundwater flow or evapotranspiration. If the groundwater levels fall, the horizon for the capillary zone will change and the upper and perhaps root zones will increase, following the sizing rules outlined in Section 2.2.3. Any new soil in the root or upper zones is assumed to have fully saturated medium pores, since it was previously in the groundwater or capillary zones. The cells with receding water table receive water left behind in the appropriate zone as groundwater levels drop, and the result will be a net increase in saturation of the medium pores in the zones if not previously fully saturated.

Root length changes: Plant growth and death may lead to a change in the root and upper zones (the capillary zone horizon is unaffected by changes in root lengths). After plants adjust their root lengths, the root and upper zones will adjust following the rules outlined in Section 2.2.3. Since we assume uniform saturation of soils within a zone, any soil that is transferred between the two zones will bring along water. The new amounts of water in a new zone are calculated based on the size of change to a zone and previous saturation levels (Appendix A).

3. Model verification and validation

To ensure that the model implementation matched its intended design, we followed three complementary verification procedures throughout model development. First, the team performed a code walk-through in which the lead programmer explained the functionality of each line of the code. This process ensured that all design concepts and specifications were correctly mapped onto the code. Second, we conducted independent verification by running portions of the whole model algorithm in a spreadsheet, checking intermediate and final outcomes (e.g., water table depth for a specific cell and date). This procedure, although time-consuming, was very effective in identifying conceptual and numerical errors, as it allowed us to compare simulation results with results from an independent system. Finally, we ran simplified but realistic scenarios to ensure that key outcomes variables had reasonable values both temporally and spatially.

We also examined how well Hydroman recreated both micro- and macro-level patterns of water table depth over time and in space (i.e., validation) (Railsback and Grimm, 2012). First, we consulted with literature and expert hydrologists to ensure that hydrological processes were adequately conceptualized and implemented in our model. Our second approach involved docking our model with other existing hydrological models that have been applied in the area of study, to see to what extent the water levels in time and space matched the ones simulated by other models. Once we established the adequacy of the model relative to existing modeling tools, we finally contrasted site-specific simulation results to observed ground and surface water records in that location. The validation process is described in more detail below.

3.1. Conceptual validation with expert hydrologists

Hydroman involves universal and well-known hydrological processes. The initial design of those processes was based on established work in hydrological modeling (Menendez and García, 2014; Mercau and Jobbágy, 2013). The main contribution of the experts was: (a) to determine which hydrological processes should be included; (b) to decide the level of detail in which each process should be represented, and (c) to simplify some key processes (e.g., soil evaporation and runoff). The involvement of local experts allowed us to keep the model simplified but relevant to its purpose.

3.2. Hydrological model docking

As a second validation technique, we aligned scenarios in Hydroman to match those in alternative established hydrological models previously used in the region. The goal of this docking exercise was to assess the extent to which Hydroman is able to reproduce temporal and spatial patterns of groundwater levels of other models (Nosetto et al., 2015). First, we performed simulations to assess the temporal dynamics of groundwater levels in one point in the space. To this end, we compared outputs from Hydroman with Hydrus-1D (Šimůnek et al., 2005) and GUARDA (Mercau and Jobbágy, 2013).[2] We also performed simulations to assess the spatial dynamics of groundwater in a two-dimensional space, comparing outputs from Hydroman with MIKE-SHE[3] (Refsgaard and Storm, 1995; Refsgaard et al., 2010). Details of this validation exercise and its results can be found in Appendix B. Overall, we observed a high degree of matching between Hydroman and both 1D and 2D models. We were also able to identify specific sources of discrepancies across models, such as the infiltration and crop transpiration used in different models, and adjust Hydroman parameters accordingly.

3.3. Validation against observed hydrological data

This assessment involved the simulation of a plot in a farm located in Pehuajó (Buenos Aires province, Argentina). We obtained monthly groundwater depth records from May 2008 to May 2013 for a 50-ha plot in this farm (Fig. 5), characterized by uneven topography and three wells located at different topographic positions of the plot (Table 1). The

[2] Hydrus 1D (PC-PROGRESS) is a public domain Windows-based modeling environment for analysis of water flow and solute transport in variably saturated porous media. GUARDA is a simplified Excel-based water budget model developed by Mercau and Jobbágy as a practical tool to simulate soil water content and groundwater depth in agricultural soils.

[3] MIKE-SHE is a deterministic, spatially-distributed, physically-based numerical model, which couples surface and groundwater flows.

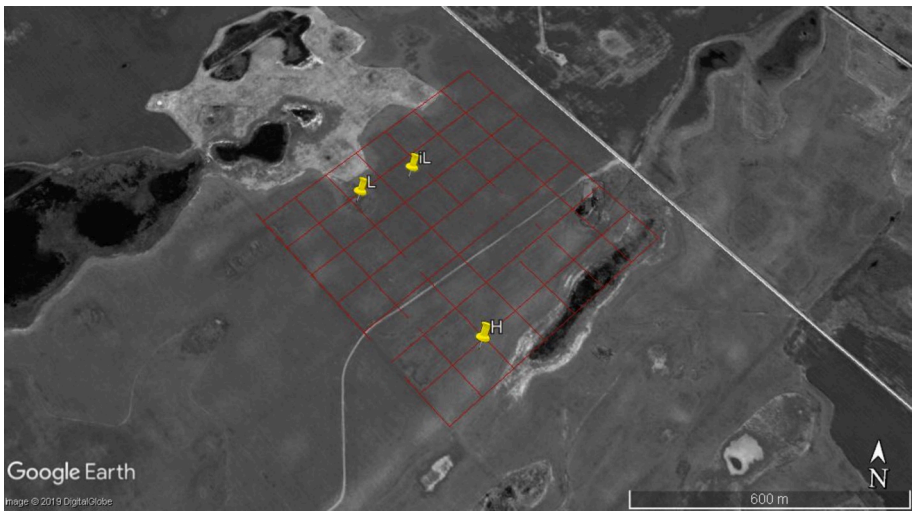

Fig. 5. Simulated Pehuajó plot and grid used for validation (source: Google Earth). The location of the three observation wells used is also indicated: high (H), intermediate-low (iL) and low (L) land.

Table 1
Characteristics of the three observation wells within the simulated plot.

Topographic position		H	iL	L
		High land	Intermediate-low land	Low land
Latitude; longitude		35°59′7.4″S; 61°45′34.92″W	35°58′52.7″S; 61°45′42.8″W	35°58′55.2″S; 61°45′47.9″W
Observed	Elevation (m.a.s.l)	93.3	91.8	91.2
	WTD May 2008 (m)	2.68	1.33	0.71
Modeled	Elevation (m.a.s.l)	90	88.5	88
	WTD May 2008 (m)	2.75	1.25	0.75

WTD: water table depth.

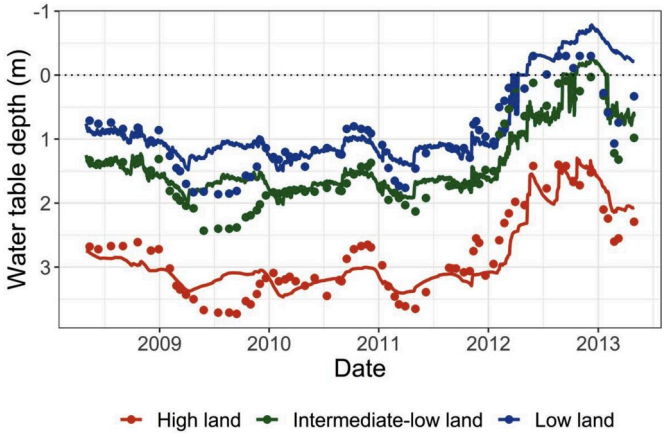

Fig. 6. Dynamics of observed (points) and simulated (lines) water table levels for the three wells located in the Pehuajó plot.

simulation aimed to recreate the groundwater dynamics at those three points during the same period.

Hydroman was set and initialized to represent as precisely as possible the plot conditions in terms of topography, soil characteristics and initial water table depth. A land surface Digital Elevation Model (DEM) based on the Shuttle Radar Topographic Mission (SRTM) was produced to represent the plot topography. A landscape with 7 × 7 cells of 1 ha each was created, and the elevation of each cell was defined based on the DEM. The DEM-based landscape roughly reproduced the topography of the plot, as confirmed by field observations. Soil-related parameter values for a typical soil in Pehuajó were assumed, and the initial water table depth at each of the observation wells was set based on records for May 2008. The sequence of land covers for the plot was also obtained, starting with cropping season 2008/09. Data from the weather station of the National Meteorological Service (SMN) in Pehuajó was used as weather input.

Hydroman was able to closely reproduce three observed structural groundwater dynamics over time (Fig. 6). The model accurately reproduced the magnitude of water table depth and the dynamics of groundwater at the three points monitored, including the significant increase towards the end of the simulated time period leading to flooding in the intermediate and lowest land. The model was able also to capture the relative differences in groundwater level between topographic positions. The model could only reproduce these patterns under closed boundary conditions that reduced the edge effects of an open fixed boundary on a small landscape. The latter introduce an artificially high supply of water that overrides any water table changes produced by the small simulated landscape.

Although Hydroman reproduced the main patterns, some second order differences (both under and over estimations) are noticeable between observed and simulated water table levels. The main differences are observed during winter-spring 2009 at the three topographic positions and towards the end of the simulation, where Hydroman tended to simulate higher water levels. We analyzed several factors that may be the source of that discrepancy. Among the most important, we included: (a) possible spatial heterogeneity in precipitations, as the simulation used data from a weather station 18 km away from the simulated farm; (b) disruption in monitoring due to a maintenance of the wells conducted during autumn 2009 which may have led to erroneous readings in the following winter; and/or (c) possible influence of groundwater levels surrounding this plot. While we assumed a closed boundary between this plot and adjacent areas to reduce edge effects, this is actually an open boundary, which may have contributed with incoming or outgoing flows.

Hydroman reproduced the crop yields registered in the Pehuajó plot in the simulated period with an acceptable precision (Fig. 7). The normalized root mean square error for all crops and cropping cycle was 18%. This is a reasonable error considering the model's parsimony, the few data points against which simulation outputs are compared, and the

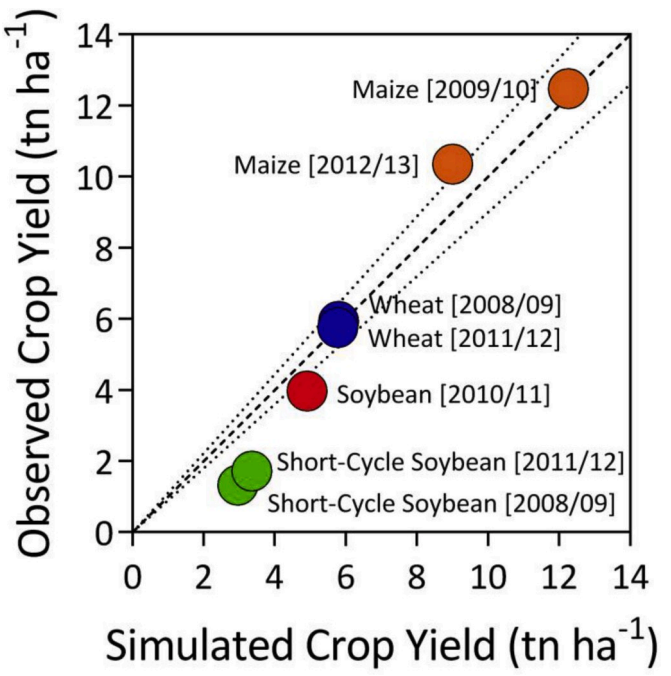

Fig. 7. Comparison between observed and simulated crop yields in the Pehuajó plot. Dashed line corresponds to the 1:1 line and dotted lines corresponds to variations of ±10%.

short time frame for the validation (5 crop rotation years). More sophisticated models like DSSAT and APSIM show similar results when applied to the Pampas region (García et al., 2018; Guevara et al., 1999; Mercau et al., 2007; Mercau and Otegui, 2014). Differences between observed and simulated yield were smaller for wheat, maize and soybean crops. Hydroman's performance was poorer only in the case of short-cycle soybean, overestimating yield for the two cropping cycles simulated. Reasons for this discrepancy may include weather extremes or biotics constraints. There was a drought in 2008/09, and heavy rains in 2011/12, which might have affected the later part of the sowing cycle. In addition, later summer crops in the Pampas usually find better water conditions during their critical periods than earlier crops. However, solar radiation levels decrease at that time, making this the main constraint on crop yield. Since Hydroman does not simulate crop yield based on radiation, the better water conditions result in an over-estimation of simulated yield. Additionally, there may have been a range of disruptions in the field that led to lower yield data.

The validation exercise above provided enough evidence that Hydroman could recreate temporal and spatial dynamics of water table consistent with those from other models and observed data, while identifying the specific sources of discrepancy. At this point, we turned to using Hydroman to explore the questions of land cover, climate, and water table interactions.

4. Understanding the influence of climate and land cover decisions on groundwater dynamics

Our goal was to use Hydroman to identify practices that may help to manage groundwater levels, contributing to a balance between preventing flooding and drought. Accordingly, we designed two sets of simulations around the following questions:

(i) How do different land cover scenarios influence water table depth?
(ii) How can adaptive land cover strategies prevent extreme water table levels?

4.1. Effect of land cover scenarios on groundwater dynamics

We seek to assess the effect of various land covers, each with different water consumption capacities, on groundwater dynamics and levels. We ran six land cover scenarios that included the typical options in the study area: (a) pasture, (b) soybean, (c) cover crop followed by soybean, (d) maize, (e) wheat followed by short-cycle soybean and (f) fallow (no crop). Land cover was the same all across the landscape and was maintained constant throughout the simulation period. Two sets of weather data were used to assess the interactions between land cover and climate: (a) three sequences, each of them generated by repeating 40 times a dry (2008/09, 542 mm), average (1980/81, 1024 mm) and wet (1986/87, 1306 mm) agricultural cycle, and (b) the historical weather records for Pehuajó (1971–2010). Further, two initial contrasting but realistic groundwater levels were simulated: 2 and 5 m to understand the influence of initial water table conditions and system behaviour towards a dynamic equilibrium. As a result, we ran 48 scenarios (6 land covers under 4 climate sequences with 2 initial groundwater levels). All scenarios assumed a completely flat landscape encompassing 11 × 11 1-ha cells for simplification purposes.

Groundwater level was strongly affected by the land cover (Fig. 8). From deeper to shallower simulated groundwater, the general order was: pasture (deepest water table depth), cover-soybean, wheat-soybean, maize, soybean, and fallow (shallowest water table depth). The deeper roots (3.5 m vs ~1.8–2 m) and the uninterrupted water consumption of pasture throughout the year led to the lowest groundwater levels in relation to the rest of the crops. Among double crops, higher water consumption during the whole agricultural cycle is evidenced when a cover crop is sown during winter. Compared to a harvest crop (i.e., wheat), the cover has an earlier plot release that allows earlier sowing and establishment of the soybean crop that follows, explaining the water consumption differences. When soybean is sown after wheat, that delay in evapotranspiration reduces its water withdrawal (Andrade et al., 2015). The wheat-soybean double crop also has little water consumption during the transition between crops (low canopy and root size) in early summer, when high atmospheric evaporative demand occurs (Mercau et al., 2016). Comparison between single crops showed groundwater levels a little deeper with maize than soybean as land cover, due to the earlier establishment and water consumption of the former during spring (maize is sown approximately one month before soybean).

The effect of land cover on groundwater dynamics heavily depended on climate scenarios and initial conditions, mostly within the first 5 to 10 simulated years until the water table reached a long-term dynamic equilibrium for most land covers (Fig. 8). Larger differences among land covers were observed under average climate conditions, with groundwater level tending to rise at different rates, except with pasture, which stabilized the water table at levels similar to dry conditions. Dry climate favored groundwater stabilization at lower depths in all land covers, rising only with fallow. Under wet conditions, groundwater tended to rise in all land covers. Initial water table depth can magnify the climate impact on groundwater dynamics at the beginning of each simulation period, further reducing differences among land covers in the extremes (i.e., dry weather and deep water table, and wet weather with shallow water table). The middle conditions (i.e. dry weather and shallow water table, average weather, and wet weather with deep water table) support more distinctive behaviors across land covers during the initial simulation period. These differences, however, disappear over time in average and wet climates.

Crop yields varied according to the climate scenario and the dynamics of groundwater (Table 2). Initial water table depth did not influence the outcomes beyond the spin up period, and results were averaged between both conditions. Under average climatic conditions, the relative yields of all land covers were closest to the maximum, showing the most favorable conditions for all crops except soybean and soybean after cover. The average scenario still introduces significant amounts of precipitation at a time that hurts the crop. Although

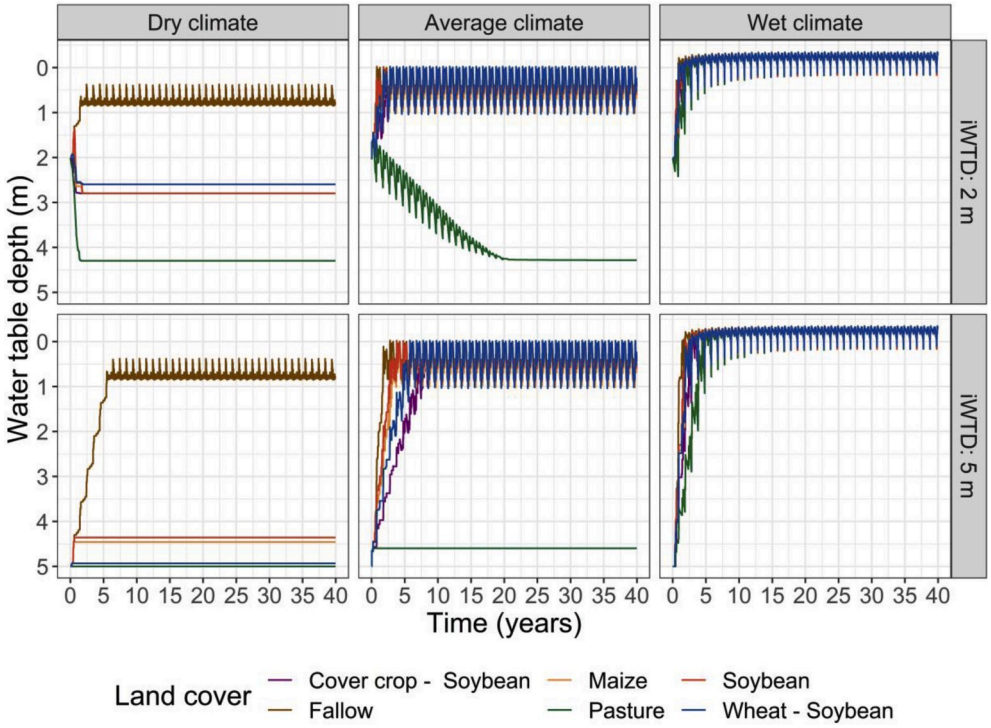

Fig. 8. Dynamics of simulated water table levels for 6 different land covers using a sequence of 40 dry, average, or wet consecutive cropping cycles for Pehuajó met station, at two initial water table depths (iWTD).

Table 2
Average crop yields (as percentage of potential yield) of the last 20 out of 40 dry, average, or wet consecutive cropping cycles simulated cycles, and of the last 20 years of the 40 years of the period simulated with historical climate for Pehuajó. Since yield differences among initial water table depths were negligible after the first 20 years for all scenarios, results were averaged between both conditions.

Climate	Land cover					
	Wheat	Soybean[a] after wheat	Soybean after cover	Soybean	Maize	Pasture
Dry	88%	50%	38%	45%	52%	52%
Average	100%	63%	0%	0%	98%	100%
Wet	0%	0%	0%	0%	0%	0%
Historical	74%	82%	80%	73%	81%	88%

[a] Short-cycle soybean.

groundwater dynamics under maize seems very similar to soybean (on average, 0.1 m deeper for maize), maize yield was high because the water table was deeper than 0.5 m during the critical crop stages. Under the sequence of wet years, the excess water decreased root functionality no matter the land cover, leading to extensive losses for all crops. Yields for most crops were also reduced under the sequence of dry years, although not to the same extent as with flooding, especially for crops with low water demand (e.g., wheat). Soybean was the most affected crop by both wet and average climate, while the others proved more robust to the range of scenarios tested. These patterns align in general with those reported by Florio et al. (2015); Mercau et al. (2016); Nosetto et al. (2015).

The results using historical climate suggest not only an interaction between land covers and total precipitation, but also among the temporal rain distribution and cover water consumption pattern. Considering the last 20 simulated years, where the initial conditions no longer influence the groundwater dynamics, the effect of water shortages or flooding determined by the actual climate variability was similar for all crops, resulting in relative yields of around 80%. Pasture had higher values and wheat and full-cycle soybean, the lower ones (Table 2). The deepest groundwater levels were observed for pasture and the shallowest for fallow, with cover-soybean and soybean as the deepest and shallowest, respectively, among the grain crops (). Groundwater dynamics both under wheat-soybean and maize had an intermediate behaviour. The differences described between those land covers in stylized scenarios (Fig. 8) are less noticeable under the historical climate series after the first few years of simulation (Fig. 9). Larger differences are observed among land covers with a deeper initial level (5 m), but only during the first half of the simulated period before the system reaches a dynamic equilibrium. Temporal variations in climate may be introducing a time lag in which crops can catch up with water uptake, maintaining overall levels below and disconnected from the surface, except where there are consecutive wet years. Overall, however, cover-soybean is better able to maintain the water table depth at more manageable levels than other land covers. A lower evapotranspiration from land cover change (i.e., the observed shift from mixed crop-cattle systems to continuous agriculture) together with increased rainfall have contributed to increase groundwater recharge in the Pampas (mainly in the area of study), favoring the rise of water tables (Aragón et al., 2011; Viglizzo et al., 2009). Although the simulations did not have this aim, the scenario with an initial water table depth of 5 m reproduced the observed groundwater patterns in the region. Under agricultural land covers, groundwater levels tended to increase, modulated by rainfall conditions. Conversely, groundwater levels stayed at deeper levels under pasture, increasing only 1 m along the 40 years of the simulation.

4.2. *Effect of adaptive land cover strategies*

Farmers have expressed interest in developing strategies to adapt to climate and water table variations (Arora et al., 2016). We extended Hydroman to represent possible adaptive strategies and to understand their effect on groundwater dynamics and risks of waterlogging on crop production. To do this, we compare scenarios in which the farmers either do not consider (non-adaptation) or consider (adaptation) water table depth to select their land cover allocation. The non-adaptive

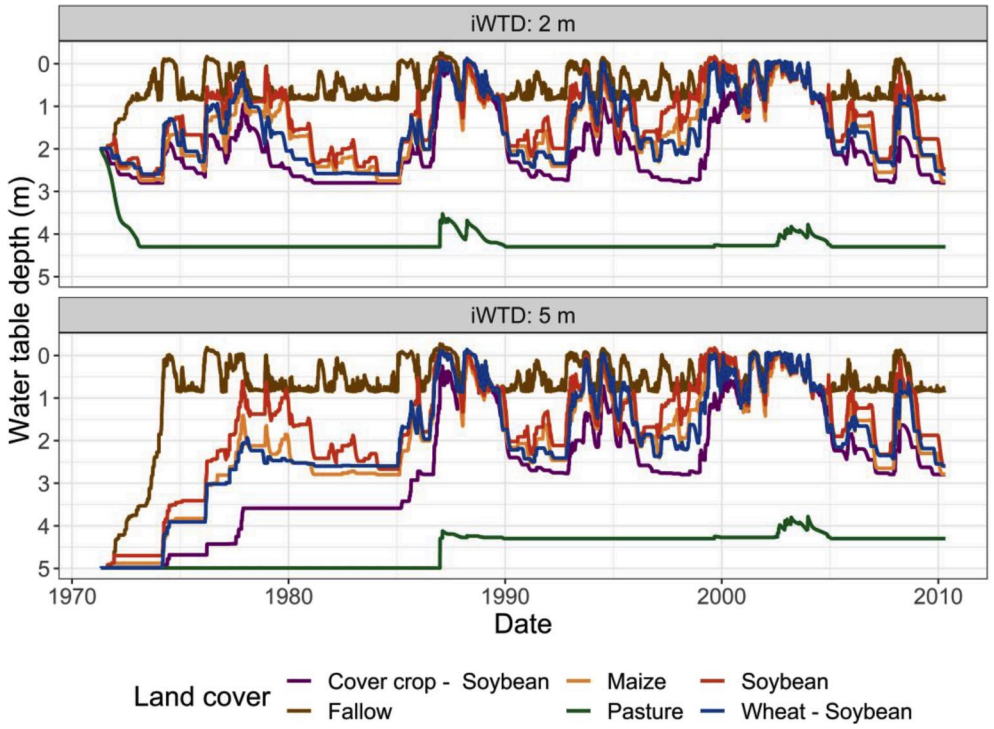

Fig. 9. Dynamics of simulated water table levels for 6 different land covers using the historical weather records (1971–2010) for Pehuajó met station, at two initial water table depths (iWTD).

strategy is characterized by a farmer who strictly followed the typical crop rotation scheme for the study area, regardless of the groundwater level (i.e., a strict rotator). Adaptive strategy, on the other hand, is characterized by farmers who decide the land cover at the beginning and throughout the cropping cycle, depending on groundwater levels regarding their reference thresholds (Fig. 10).

The default rotation sequence, which is adopted by the strict rotator (non-adaptive strategy) is maize (Year 1), full-cycle soybean (Year 2), and wheat or cover crop followed by soybean (short- or full-cycle soybean, respectively) (Year 3). Adaptive farmers would deviate from this sequence depending on water table depth at the moment of sowing decisions. The rationale behind the adaptive strategy represented in the

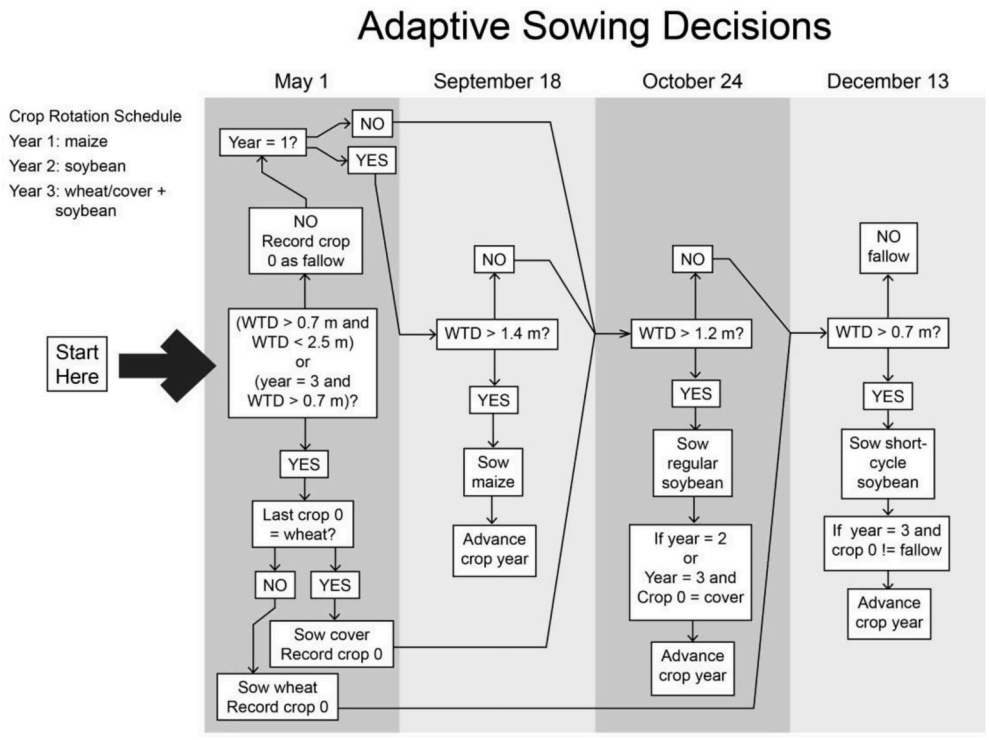

Fig. 10. Adaptive strategy simulated. Land cover decisions rules followed by farmers based on water table depth readings (threshold values are indicated) at different times of the cropping cycle.

model is that the farmer may introduce a high consumption cover to lower water table levels under threatening waterlogging conditions. Groundwater thresholds assumed by farmers correspond to the lower limit of optimal depth range for highest yield for wheat, maize and soybean (0.7, 1.4 and 1.2 m, respectively) (Nosetto et al. (2009).

Thus, on May 1 (day 0) of each year during a simulation, if (a) the water table depth is between the shallow and deep thresholds, or (b) it is Year 3 in the rotation and the depth to the water table is greater than the shallow thresholds, wheat will be sown if it wasn't sown the previous year. Otherwise, cover crop will be sown, assuming farmers would allow soil recovery by rotating crops. The farmer will recheck the water table depth on December 13 after sowing wheat, or on October 24 after sowing cover crop, to determine if a subsequent sowing happens. However, if conditions a) or b) above are not met, the farmer will not sow in May, and will recheck the water table on September 18 if it is Year 1 in the crop rotation (corresponding to the sowing of maize), or on October 24 any other year. If marked to recheck the water table depth on September 18 and on that day the water table depth is deeper than the threshold, the farmer will sow maize and advance the rotation year. If shallower than the threshold, the farmer will recheck on October 24. By that date, those farmers marked to check the water table depth will sow full-cycle soybean if the water table is deeper than the threshold. Also, if it is Year 2 of the rotation, or Year 3 of the rotation and a cover crop was sown on May 1, the rotation year advances. If the water table was not deep enough to allow any crop sowing in October, the farmer will check again the water table depth on December 13. On December 13 (the final opportunity to check the water table during a cropping cycle), if the water table is deeper than the threshold, short-cycle soybean will be sown. If it is Year 3 of the rotation and either wheat or cover had been sown on May 1, the rotation year is reset to Year 1. If the water table was shallower than the threshold on this day, the land will remain fallow. The famer decisions are all represented at the cell level.

The experiment included the two decision strategies described above, adopted in two landscapes: a completely flat, stylized landscape, and the plot from Pehuajó used for model validation (Section 3.3). The landscape encompasses 7 × 7 cells of 1 ha each in both cases, always under the historical weather records (1971–2010) from the Pehuajó weather station and starting in an initial groundwater level of 2 m. Additionally, two precision levels in the water table depth readings were adopted to guide land cover decisions in the Pehuajó landscape: low (sowing decisions in each cell are based on groundwater levels from a single cell in the entire plot), or high (decisions are based on groundwater levels in each cell in the plot). In the low precision level all the cells in the plot will have the same land cover, while in the high precision level each cell will have a land cover according to its groundwater level.

The water table depth results suggest several trends (Fig. 11). The bimodal distribution in water table depth is in line with theoretical discussions in our broader research team, prompted by field observations. There are essentially two basins of attraction for the water table, represented in the two peaks in the distribution of the Pehuajó landscape. The depth of these two basins depends heavily on the crop's root length and transpiration rates. Under normal or dry conditions, transpiration depresses the water table only as much as its root length allows. Water levels will rise with precipitation, but transpiration will keep them in that basin. When a wet period causes a significant rise in the water table and consumption cannot keep up, the roots are killed due to anoxia, decreasing the capacity of the plant to transpire and exacerbating the water table rise. Once it reaches the surface, direct evaporation takes over, operating at greater rates to compensate for rising water levels. This then becomes the second basin of attraction. In contrast with the Pehuajó landscape, a flat landscape minimizes the lateral flows afforded by heterogeneous elevations, increasing the sensitivity to different root lengths.

Among the sowing strategies, adaptation is better able to maintain the water table at lower depths than strict rotation when the landscape is flat (i.e., cells have complete information about the landscape). Widespread sowing of specific crops that affect the water table depth can have a substantial impact on keeping the water table at desirable levels, even when climate is unfavorable. At the other extreme, when cells make decisions on one point in a heterogeneous landscape, adaptation is worse than strict rotation. That is, for adaptation to be successful, it must rely on appropriate levels of information; otherwise, the wrong crops will be sown in the wrong places. Initial sensitivity tests on water table depth thresholds showed that adaptation matters more than the details of its implementation, and is a robust strategy when information is available to maintain the water table at acceptable levels.

In heterogeneous landscapes and more decentralized decision-making (i.e., when each cell decides its own sowing), we see virtually the same outcomes between adaptation and strict rotation (Fig. 11). This suggests that the temporal variability brought about by strict rotation can partially compensate for the fluctuations in water table depth that each cell experiences. Adaptation can compensate for spatial differences over a single time period, by adapting to geographic differences in water table depths at one time. Strict rotation, on the other hand, can compensate for differences in water table depth across time periods so that a water-demanding crop can help address high water tables left over by less water-demanding crops.

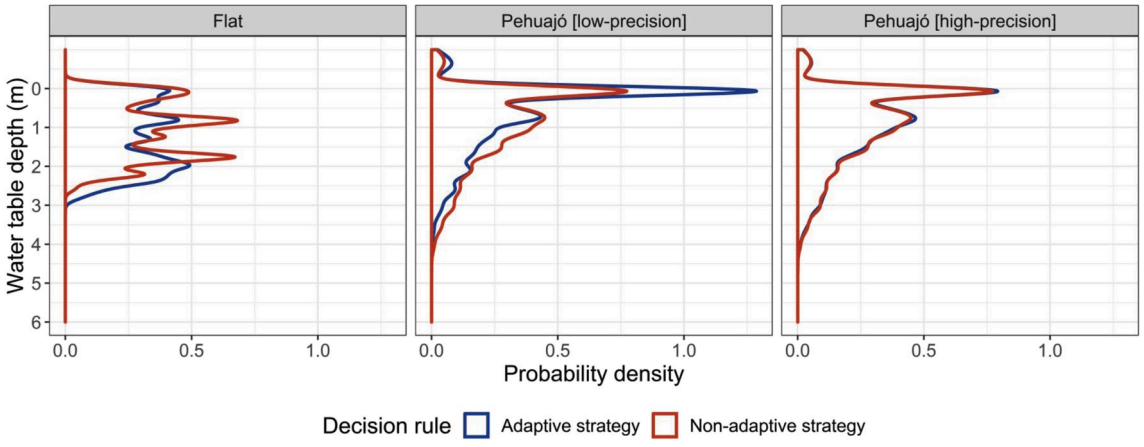

Fig. 11. Water table depth under different land cover decision rules in different landscapes and/or decisions precision. Probability density curves of water table depth along the last 19 out of 39 cycles in which adaptive or non-adaptive (strict rotator) strategies were applied to a 49 ha landscape: flat or Pehuajó. In the low precision level, all the cells in the plot adopt the same land cover, while in the high precision level each cell adopts a land cover according to its groundwater level. The difference in decision precision occurs only in the Pehuajó landscape, as in the flat landscape all cells have the same groundwater level.

Overall, adaptation seems to be a robust strategy to follow in homogeneous landscapes, but precision agriculture might be important in ensuring its success in more heterogeneous landscapes. Adaptive strategies may end up with more instances of fallow cover in heterogeneous landscapes with low information levels, exacerbating flooding (Table 3). This effect could be countered if, instead of leaving land fallow, flood-resistant crops were sowed. Strict rotators do not allow their land to go fallow (non-crop), and thus may better maintain the water levels below the surface, although exposing themselves to more losses due to flooding.

In relation to crop yields, simulations tend to show that adaptation may still be overall better than strict rotation (Table 3). Particularly when we observe crop losses, a pattern emerges of how adaptation provides an advantage over strict rotation. Risk averse loses fewer crops than strict rotators. Because strict rotators do not consider water table depth, they end up losing more of their crops mostly to flooding, although they may also do so to drought. They can partially compensate for these losses, however, by sowing at risk, which sometimes may turn out well for them, especially when it helps lower water table levels. Paradoxically, by adapting to water table levels, adaptive decision-makers increasingly avoid sowing and thus exacerbate the flooding problem. Yields may be higher for the land farmed and losses may be minimized, but the areas farmed are much smaller.

Given these results, we hypothesized that re-introducing pasture to the flat lands might be beneficial in regulating water table depths and thus ensure more successful outcomes, particularly since the cost of farming and monitoring water levels at high precision would be unrealistically costly. Confirming our expectations, the inclusion of pasture in the heterogeneous Pehuajó landscape improved the performance of the system by increasing crop yields, reducing crop losses, and stabilizing the water table (Table 3 and Fig. 12). Introducing as little as 7 random cells of pasture over the 49 (14% coverage) slightly increased the yield of all strategies and reduced the crop losses. Moreover, less land is left fallow in the adaptive strategies. At double that area of pasture (29% coverage), yield increased and crop losses were further reduced. Sowing 21 cells of pasture (43% coverage) stabilized the water table depth, increasing the benefits for the strict rotator by reducing crop losses and increasing yields to levels similar to the risk averse, virtually eliminating the advantage of adaptation (and the associated monitoring cost). At this point, however, pasture started occupying half of the lot, severely competing for space. It is also worth noting that none of these conditions trigger the sowing of maize in the adaptive decision-making, suggesting that water levels may still be too high for this crop. These results imply that a stabilizing longer term strategy that allocates pasture in different spatial arrangements may be worth exploring in more detail, relative to the use of flood-resistant crops when crises arise.

Table 3
Summary of yields for different land cover decision rules applied over the last 19 out of 39 years in the Pehuajó plot (low precision), varying pasture allocation. Crop allocation: percentage of the total possible area (i.e., 49 ha multiplied by 19 years), crop production: average yield of the crop as percentage of its potential yield, crop loss: percentage of area allocated to the crop where yield was 0.

Pasture allocation	Crop	Crop allocation (% of total area)		Production (% of potential)		Crop loss (% area with yield = 0)	
		A	NA	A	NA	A	NA
0%	Cover	–	–	–	–	–	–
	Wheat	15.8	31.6	80.5	72.5	12.9	23.5
	Maize	–	31.6	–	62.4	–	28.2
	Soybean	–	36.8	–	69.2	–	21.0
	Short soybean	21.1	31.6	78.6	66.4	12.8	24.1
	Pasture	–	–	–	–	–	–
	Non-crop	68.4	–	–	–	–	–
14%	Cover	4.5	–	85.8	–	11.9	–
	Wheat	13.5	27.1	85.5	78.0	7.1	17.5
	Maize	–	27.1	–	68.1	–	23.4
	Soybean	–	31.6	–	73.7	–	14.6
	Short soybean	22.6	27.1	79.7	73.3	12.4	16.3
	Pasture	14.3	14.3	34.9	48.3	0.0	0.0
	Non-crop	58.6	–	–	–	–	–
29%	Cover	3.8	–	95.5	–	2.9	–
	Wheat	11.3	22.6	91.6	85.2	1.9	11.0
	Maize	–	22.6	–	75.9	–	13.8
	Soybean	–	26.3	–	79.0	–	8.6
	Short soybean	22.6	22.6	84.5	82.4	6.2	10.5
	Pasture	28.6	28.6	41.9	54.5	0.0	0.0
	Non-crop	48.9	–	–	–	–	–
43%	Cover	24.1	–	90.1	–	4.5	–
	Wheat	24.1	18.0	86.5	91.1	2.2	4.2
	Maize	–	18.0	–	83.9	–	6.5
	Soybean	15.0	21.1	87.4	82.3	0.0	3.6
	Short soybean	36.1	18.0	87.7	90.1	4.8	5.4
	Pasture	42.9	42.9	63.5	62.8	0.0	0.0
	Non-crop	6.0	–	–	–	–	–

A: adaptive strategy, NA: non-adaptive strategy (strict rotator).

5. Implications for agricultural decision-making

We developed a parsimonious, process-based, dynamic and spatially explicit model, called Hydroman, that considers the main hydrological processes of groundwater and surface water flow, as a function of land cover and climate. Hydroman provides a flexible platform to quickly and easily examine how the human dimension of agriculture (sowing decision rules) influence both water table levels and crop yields in flat agricultural areas. The model was able to reproduce patterns of groundwater levels over time and in space, capturing both the micro-level complexity (as validated by experts in the field) and the emerging macro-level patterns (as validated by alignment with established models and empirical data). We used Hydroman to understand how climate, land cover and water tables interact, and with this understanding, identify possible strategies for agricultural water management.

While climate continues to be a main driver in the system, the switch from cattle ranching to annual grain crops, which use less water than pasture, has also influenced the water balance of the region (Nosetto et al., 2012; Viglizzo et al., 2009). Among the land covers examined, double crops tend to reduce the now predominant risk of flooding by extending the period of time in which they absorb water. However, it may be more difficult to plant it in areas that are already waterlogged.

Adaptive strategies offer some relief from flooding, but only if implemented with spatial precision. With more spatial variability, the advantages disappear and even may backfire, as sowing is adapting to the wrong information, thus increasing the risk of lower yields, greater losses, and flooding. With appropriate information, the details of adaptation matter less than the fact that environmental information is being used to make decisions. When information is lacking, strict rotation may, in fact, be the better option, particularly with increasing landscape heterogeneity. In extreme years, however, adaptation may not be enough to prevent flooding, particularly when sowing is avoided to minimize losses, which exacerbates the flooding problem. Policy makers and farmers may wish to consider a partial reversal to pasture, strategically locating them in low-lying areas, in enough coverage to generate more stability in the system.

Hydroman is set up in a way that allows for further development and exploration of management strategies. Among the ones we seek to explore in future work are rules that account for decision in neighboring plots, which poses a coordination problem among actions that can potentially exacerbate or cancel out effects. Such explorations would allow us, for example, to develop generalizable recommendations for the allocation (amount and spatial location) of pasture to reduce flooding risk. Such decisions, however, may have different implications

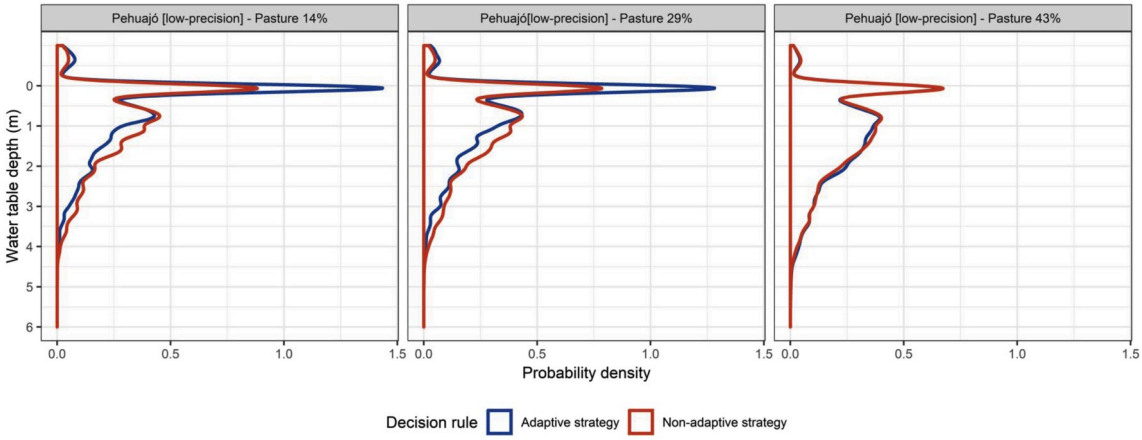

Fig. 12. Water table depth under different land cover decision rules in the Pehuajó landscape with low precision decision and variable pasture area allocation. Probability density curves of water table depth for the last 19 out of 39 cycles of adaptive or non-adaptive (strict rotator) strategies in a 49 ha landscape, where 7 (14%), 21 (29%) or 21 (43%) hectares are allocated to pasture.

for the distribution of benefits and losses of the actors in the system. To pursue this work, we will work with stakeholders, to both develop strategies and to examine them in an iterative participatory modeling process. Collaborative approaches supported by flexible and parsimonious models like Hydroman can support the emergence of new institutions that can increase the adaptive capacity, resilience and sustainability of human-natural systems, beyond the agricultural settings we represent here (Gray et al., 2018; Voinov et al., 2018; Zellner, 2008; Zellner et al., *in press;* Zellner et al., 2012).

Software availability

Name of software: Hydroman.
Developers: Dean Massey and Moira Zellner
Contact information: mzellner@uic.edu
Hardware required:
Software required: NetLogo.
Programming languages: NetLogo.
License: www.comses.net/codebase-release/1db4c97d-46f1-42dd-9d62-77bf45f95776/.

Declaration of competing interest

The authors declare that they have no known competing financial interests or personal relationships that could have appeared to influence the work reported in this paper.

Acknowledgements

This work was supported by the National Science Foundation (NSF) CNH Award #1211613, the UIC Under-Represented Faculty Recruitment Program co-sponsored by the Provost and the College of Urban Planning and Public Affairs, CONICET Argentina (PIP 112-201501-00609), ANPCyT Argentina (PICT 2014–2790 and 2017–3811), and the Inter-American Institute for Global Change Research (IAI) grant CRN-3035 (in turn supported by the NSF grant GEO-1128040). Guillermo Garcia held a postdoctoral fellowship from the National Scientific and Technical Research Council (CONICET, Argentina). We greatly appreciate the support of G. Podestá, Principal Investigator of this grant, and early conversations with Co-Investigators P. Arora, B. Rajagopalan and C. Macal. We are very thankful to E. Jobbagy, J. Mercau, A. Menéndez and P. García for their contribution in the conceptual validation of Hydroman, and S. Rovere for assistance with R scripts.

Appendix A. Example calculation of water transfer across soil horizons

We illustrate with an example below the calculations that update soil horizons in Hydroman and transfer the corresponding water content across horizons as they change. In this illustrative example, the code updates the root and upper zones after the daily growth of the root.

1. Calculate the new lower limit of the root zone

Equation A1	Example
$if\ S - T_c > 0.3\ and\ S - T_c > L$	$10 - 9 > 0.3$ and $10 - 9 > 0.5$

Where:

S = the elevation of the cell, in m
T_c = The depth to the capillary zone, in m
L = the length of the roots, in m

1.1. If true

Equation A1.1	Example
$B_{r,t+1} = S - \max(0.3; L)$	$B_{r,t+1} = 9.495 = 10 - 0.505$

Where:

$B_{r,t}$ = the root zone lower limit at time t, in m

1.2. If false

Equation A1.2	Example
$B_{r,t+1} = T_c$	Not applicable

2. Determine the size of the change to the root zone

Equation A2	Example
$\Delta C_r = C_{r,t+1} - C_{r,t}$	$\Delta \mathrm{Cr} = 0.005 = 0.505 - 0.5$

Where.

$C_{r,t}$ = the height of the root zone soil column at time t, in m

3. If there is a change in the root zone

3.1. If the change is positive, soil and water content must be transferred from the upper zone to the root zone

3.1.1. Determine the water content of the upper zone (amount there/maximum there)

Equation A3.1.1	Example
$\theta_u = W_{u,t}/(C_{u,t} \times e_m)$	$0.75 = 0.045/(0.5 \times 0.12)$

Where:

Θ_u = the water content of the medium pores in the upper zone, in % saturation
$W_{u,t}$ = the height of the water column in the upper zone at time t, in m
$C_{u,t}$ = the height of the upper zone soil column at time t, in m
e_m = the medium pore specific yield (% porosity)

3.1.2. Determine the change to the upper zone's water column

Equation A3.1.2	Example
$\Delta W_u = \lvert\Delta C_r\rvert \times \theta_u \times P_m$	$0.00045 = \lvert 0.005\rvert \times 0.75 \times 0.12$

Where:

ΔW_u = the change in height of the upper zone water column in m

3.1.3. Transfer the water from the upper zone to the root zone and adopt the updated values for soil horizons

3.2. If the change is negative, soil and water content must be transferred from the root zone to the upper zone same as above, but with transfers from the root zone to the upper zone.

Appendix B. Comparison of Hydroman with other hydrological models

B1. Temporal dynamics of groundwater

The evolution of groundwater depth under different climate scenarios and initial groundwater levels was simulated with Hydroman and two alternative one-dimensional (vertical) hydrological models: Hydrus-1D and GUARDA. Hydrus 1D (PC-PROGRESS) is a public domain Windows-based modeling environment for analysis of water flow and solute transport in variably saturated porous media (Šimůnek et al., 2005), which has been used in the study area to simulate groundwater dynamics (Nosetto et al., 2015). GUARDA is a simplified Excel-based water budget model developed by Mercau and Jobbágy (2013) as a practical tool to simulate soil water content and groundwater depth in agricultural soils.

Simulations were performed using weather records and soil parameters from Pehuajó, a representative location in the study area. A landscape with 11 × 11 cells of 1 ha each was created. It was assumed to be completely flat, and the watershed was entirely contained within the landscape. All simulations spanned an agricultural cycle (from May 1st of year 0 to Apr 31st of year 1). Three different agricultural cycles were selected from the historical climate records according to total precipitations to perform simulations under dry (2008/09, 542 mm), average (1980/81, 1024 mm) and wet (1986/87, 1306 mm) agricultural cycles. The land cover assumed for all simulations was soybean for the whole landscape. These three climate scenarios were combined with three initial (May 1st) groundwater depths: 0.5, 2.0 and 3.5 m. Simulated daily water table depth from each model was compared. Because Hydroman is not a 1D model, groundwater levels at the center cell were analyzed to make the runs comparable across models.

The water table dynamics simulated by Hydroman were very similar to that simulated by the other two models for most of the situations (Fig. B1). This similarity suggests that Hydroman captures the main hydrological processes that reproduce the dynamic patterns. There were differences between the models in some cases, specifically between Hydroman and GUARDA (Fig. B1, middle panel). The differences can be tied to how each model

represents some key hydrological processes. For instance, while GUARDA uses the empirical curve number approach to represent runoff, this process is endogenously simulated in Hydroman and Hydrus. As a result, while in GUARDA there is always runoff, Hydroman does not produce runoff when the landscape is completely flat and the land cover is homogenous. Hydroman will produce runoff in heterogeneous landscape, either for land cover or topography.

To evaluate if differences between Hydroman and GUARDA were associated with the infiltration process, effective rainfall[4] simulated by GUARDA was used as input data to Hydroman. The outputs from these simulations were much closer (Fig. B2).

Although Hydroman produced results very similar to Hydrus, the latter produced smoother trajectories of water table levels, mainly for deep initial water table depth (e.g., left lower panel, Fig. B1). The difference in the dynamics of simulated water table may be tied to the way in which each model simulates vertical fluxes. Hydroman considers a "cascade" model and Hydrus relies on Richard's approach. The conductivity approach tends to smooth trajectories, especially when the soil layer above water table is wide.

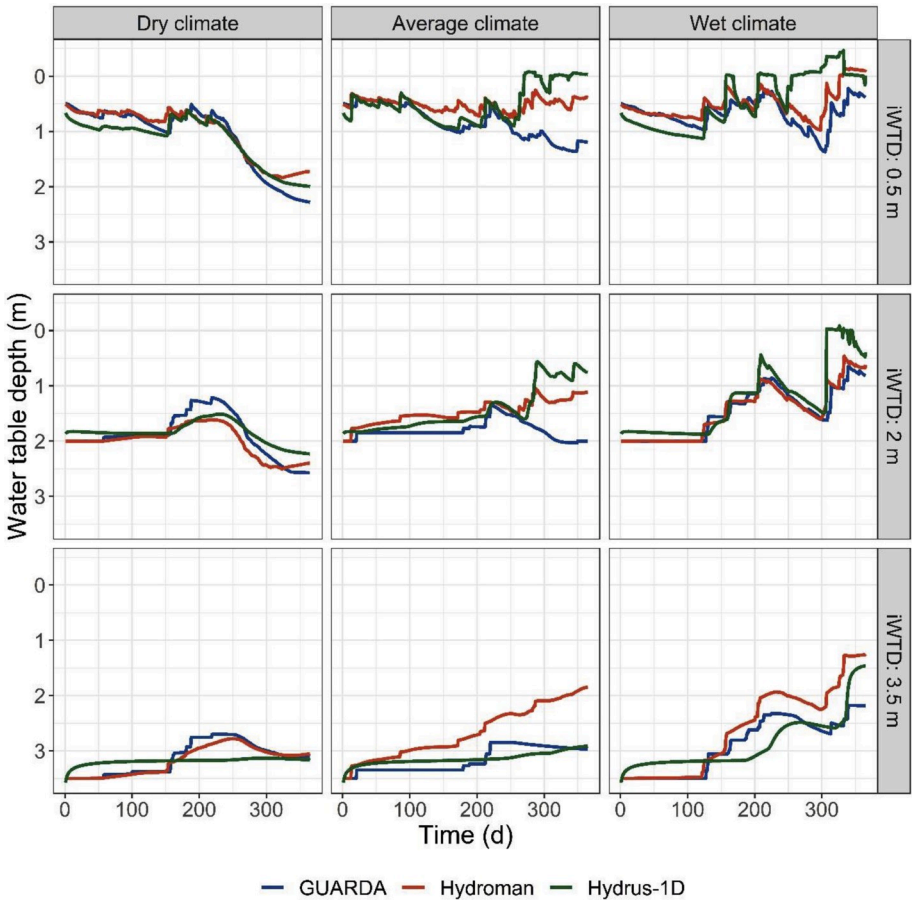

Fig. B1. Temporal dynamics of groundwater simulated by GUARDA, Hydroman and Hydrus-1D in 9 scenarios resulting from the combination of rainfall amounts during the agricultural cycle (dry, average or wet climate) and initial water table depth (0.5, 2 or 3.5 m).

[4] Rainfall stored in the root zone that can be use by plants (i.e., water not lost by deep percolation and/or run-off).

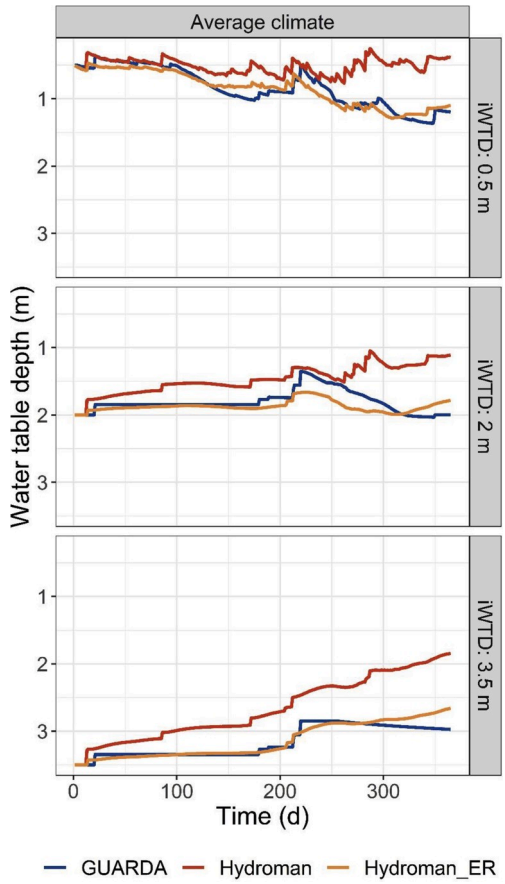

Fig. B2. Temporal dynamics of groundwater simulated with GUARDA and Hydroman with two alternative inputs: (i) normal or (ii) effective rainfall from GUARDA (to compare with it), in 3 scenarios resulting from the combination of average rainfall amounts during the agricultural cycle and initial water table depth (0.5, 2 or 3.5 m).

B2. Spatial dynamics of groundwater

The spatial dynamics of groundwater within a simplified landscape was simulated with Hydroman and MIKE-SHE models. MIKE-SHE is a deterministic, spatially-distributed, physically-based numerical model, which couples surface and groundwater flows (Refsgaard and Storm, 1995; Refsgaard et al., 2010). This model had been calibrated and validated in the study area (Badano, 2010; García et al., 2017, 2019). Our simulations were specifically aimed to assess spatial variations in water table depth as result of horizontal water flows triggered by heterogeneous land uses, i.e. with contrasting water consumption, over the landscape.

The simulated landscape involved a square grid of 151 × 151 cells of 1 ha each cell. The land cover assigned to the whole landscape was soybean except for an island of 31 × 31 cells at the center that was assigned to pasture, a land cover with higher water consumption. The simulation was performed using an average rainfall year (1981/82) for Pehuajó, also with a completely flat landscape. Soil-related parameters were defined for each model to represent a typical soil in Pehuajó. The initial water table depth was set to 2.5 m in both models. Water table depth from each model lengthwise in the landscape was compared at the end of the season (Apr 30th, 1982).

Hydroman was able to simulate spatial changes in groundwater levels in response to heterogeneous land covers (pasture and soybean), that were qualitatively similar to those produced by MIKE-SHE (Fig. B3). These different groundwater levels were triggered by the response to differential water uptake between two plant covers. Although the spatial pattern of water table levels was qualitatively similar between models, there were quantitative differences in water table depth by the end of the simulation. We hypothesized that these differences were likely associated with a variety of processes that differ in their representation in each model. For instance, crop transpiration is represented via the k_{cb} coefficient in Hydroman and via the Leaf Area Index in MIKE-SHE. Similarly, some parameters characterizing soil properties and initial conditions are different in each model, which prevent a perfect alignment between models. Although we could calibrate Hydroman to close the gap with MIKE-SHE outcomes by manipulating any of these variables, we decided to maintain the original setting, because our focus was on assessing relative spatial patterns and not in reproducing absolute groundwater levels.

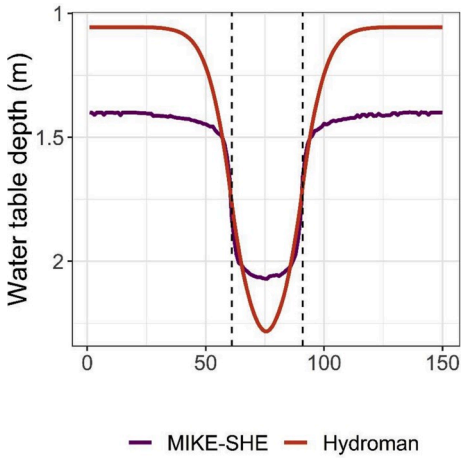

Fig. B3. Groundwater levels simulated by Hydroman and MIKE-SHE on a longitudinal section of the landscape. The dashed lines mark the limits of the central island planted with pasture; the rest of the landscape is planted with soybean.

Appendix C. Supplementary data

Supplementary data to this article can be found online at https://doi.org/10.1016/j.envsoft.2020.104641.

References

Allen, R.G., Pereira, L.S., Raes, D., Smith, M., 1998. Crop Evapotranspiration: Guidelines for Computing Crop Water Requirements. FAO, Rome, Italy. FAO Irrigation and Drainage Paper No. 56.

Andrade, J.F., Poggio, S.L., Ermácora, M., Satorre, E.H., 2015. Productivity and resource use in intensified cropping systems in the Rolling Pampa, Argentina. Eur. J. Agron. 67, 37–51.

Aragón, R., Jobbágy, E.G., Viglizzo, E.F., 2011. Surface and groundwater dynamics in the sedimentary plains of the Western Pampas (Argentina). Ecohydrology 4 (3), 433–447.

Arora, P., Peterson, N.D., Bert, F., Podesta, G., 2016. Managing the triple bottom line for sustainability: a case study of Argentine agribusinesses. Sustain. Sci. Pract. Pol. 12 (1), 60–75.

Badano, N., 2010. Modelación integrada de grandes cuencas de llanura con énfasis en la evaluación de inundaciones. Facultad de Ingeniería. Universidad de Buenos Aires, Buenos Aires, Argentina, p. 158.

Berbery, E.H., Doyle, M.E., Barros, V., 2006. Tendencias regionales en la precipitación. In: Barros, V., Clarke, R., Silva Días, P. (Eds.), El cambio climático en la Cuenca del Plata, first ed. CIMA-CONICET, Buenos Aires, pp. 61–73.

Bert, F.E., Rovere, S.L., Macal, C.M., North, M.J., Podestá, G.P., 2014. Lessons from a comprehensive validation of an agent based-model: the experience of the Pampas Model of Argentinean agricultural systems. Ecol. Model. 273, 284–298.

Boulanger, J.-P., Leloup, J., Penalba, O., Rusticucci, M., Lafon, F., Vargas, W., 2005. Observed precipitation in the Paraná-Plata hydrological basin: long-term trends, extreme conditions and ENSO teleconnections. Clim. Dynam. 24 (4), 393–413.

Calviño, P., Monzon, J., 2009. Farming systems of Argentina: yield constraints and risk management. In: Sadras, V., Calderini, D. (Eds.), Crop Physiology. Academic Press, San Diego, pp. 55–70.

Calviño, P., Sadras, V., 2002. On-farm assessment of constraints to wheat yield in the south-eastern Pampas. Field Crop. Res. 74 (1), 1–11.

Calviño, P.A., Andrade, F.H., Sadras, V.O., 2003. Maize yield as affected by water availability, soil depth, and crop management. Agron. J. 95 (2), 275–281.

Castilla-Rho, J.C., Mariethoz, G., Rojas, R., Andersen, M.S., Kelly, B.F.J., 2015. An agent-based platform for simulating complex human–aquifer interactions in managed groundwater systems. Environ. Model. Software 73, 305–323.

Dardanelli, J.L., Bachmeier, O.A., Sereno, R., Gil, R., 1997. Rooting depth and soil water extraction patterns of different crops in a silty loam Haplustoll. Field Crop. Res. 54 (1), 29–38.

Fan, Y., Li, H., Miguez-Macho, G., 2013. Global patterns of groundwater table depth. Science 339 (6122), 940–943.

Florio, E.L., Mercau, J.L., Nosetto, M.D., 2015. Factores que regulan la dinámica freática en dos ambientes de la Pampa Interior con distintos regímenes de humedad. Cienc. del Suelo 33 (2), 263–272.

García, G.A., García, P.E., Rovere, S.L., Bert, F.E., Schmidt, F., Menéndez, Á.N., Nosetto, M.D., Verdin, A., Rajagopalan, B., Arora, P., Podestá, G.P., 2019. A linked modelling framework to explore interactions among climate, soil water, and land use decisions in the Argentine Pampas. Environ. Model. Software 111, 459–471.

García, G.A., Miralles, D.J., Serrago, R.A., Alzueta, I., Huth, N., Dreccer, M.F., 2018. Warm nights in the Argentine Pampas: modelling its impact on wheat and barley shows yield reductions. Agric. Syst. 162, 259–268.

García, P.E., Menéndez, A.N., Podestá, G., Bert, F., Arora, P., Jobbágy, E., 2017. Land use as possible strategy for managing water table depth in flat basins with shallow groundwater. Int. J. River Basin Manag. 1–14.

Gleeson, T., Wada, Y., Bierkens, M.F.P., van Beek, L.P.H., 2012. Water balance of global aquifers revealed by groundwater footprint. Nature 488 (7410), 197–200.

Goddard, L., Mason, S.J., Zebiak, S.E., Ropelewski, C.F., Basher, R., Cane, M.A., 2001. Current approaches to seasonal to interannual climate predictions. Int. J. Climatol. 21 (9), 1111–1152.

Gray, S., Voinov, A., Paolisso, M., Jordan, R., BenDor, T., Bommel, P., Glynn, P., Hedelin, B., Hubacek, K., Introne, J., Kolagani, N., Laursen, B., Prell, C., Schmitt Olabisi, L., Singer, A., Sterling, E., Zellner, M., 2018. Purpose, processes, partnerships, and products: four Ps to advance participatory socio-environmental modeling. Ecol. Appl. 28 (1), 46–61.

Guevara, E., Meira, S., Maturano, M., Coca, M.G., 1999. Maize simulation for different environments in Argentina. In: International Symposium: Modelling Cropping Systems. European Society of Agronomy, Lleida, Spain, pp. 193–194.

Hall, A.J., Rebella, C.M., Ghersa, C.M., Culot, J.P., 1992. Field-corp systems of the pampas. In: Pearson, C.J. (Ed.), Field Crop Ecosystems: Ecosystems of the World. Elsevier, Amsterdam, Holland, pp. 413–450.

Jalota, S.K., Prihar, S.S., 1990. Bare-soil evaporation in relation to tillage. In: Stewart, B. A. (Ed.), Advances in Soil Science. Springer-Verlag, New York, USA, pp. 187–216.

Jobbágy, E.G., Jackson, R.B., 2004. Groundwater use and salinization with grassland afforestation. Global Change Biol. 10, 1299–1312.

Jobbágy, E.G., Nosetto, M.D., Santoni, C.S., Baldi, G., 2008. El desafío ecohidrológico de las transiciones entre sistemas leñosos y herbáceos en la llanura Chaco-Pampeana. Ecol. Austral 18, 305–322.

Jones, J.W., Hoogenboom, G., Porter, C.H., Boote, K.J., Batchelor, W.D., Hunt, L.A., Wilkens, P.W., Singh, U., Gijsman, A.J., Ritchie, J.T., 2003. The DSSAT cropping system model. Eur. J. Agron. 18 (3–4), 235–265.

Kang, S., Zhang, F., Hu, X., Jerie, P., Zhang, L., 2001. Effects of shallow water table on capillary contribution, evapotranspiration, and crop coefficient of maize and winter wheat in a semi-arid region. Aust. J. Agric. Res. 52 (3), 317–327.

Langevin, C.D., Hughes, J.D., Banta, E.R., Provost, A.M., Niswonger, R.G., Panday, S., 2018. MODFLOW 6 Modular Hydrologic Model, Version 6.0.3: U.S. Geological Survey Software Release, 9 August 2018.

Menendez, A.N., García, P.E., 2014. Laboratorio de Hidráulica. Instituto Nacional Del Agua, Ezeiza, Argentina.

Mercau, J.L., Dardanelli, J.L., Collino, D.J., Andriani, J.M., Irigoyen, A., Satorre, E.H., 2007. Predicting on-farm soybean yields in the pampas using CROPGRO-soybean. Field Crop. Res. 100 (2–3), 200–209.

Mercau, J.L., Jobbágy, E.G., 2013. GUARDA: Guía para el Uso del Agua y sus Riesgos en Decisiones Agrícolas. Grupo de Estudios Ambientales, Instituto de Matemática Aplicada San Luis, CONICET & Universidad Nacional de San Luis: San Luis, Argentina.

Mercau, J.L., Nosetto, M.D., Bert, F., Giménez, R., Jobbágy, E.G., 2016. Shallow groundwater dynamics in the Pampas: climate, landscape and crop choice effects. Agric. Water Manag. 163, 159–168.

Mercau, J.L., Otegui, M.E., 2014. A modeling approach to explore water management strategies for late-sown maize and double-cropped wheat–maize in the rainfed pampas region of Argentina. In: Ahuja, L.R., Ma, L., Lascano, R.J. (Eds.), Practical Applications of Agricultural System Models to Optimize the Use of Limited Water. American Society of Agronomy, Inc., Crop Science Society of America, Inc., and Soil Science Society of America, Inc., pp. 351–374

Mueller, L., Behrendt, A., Schalitz, G., Schindler, U., 2005. Above ground biomass and water use efficiency of crops at shallow water tables in a temperate climate. Agric. Water Manag. 75 (2), 117–136.
Negm, L.M., Youssef, M.A., Skaggs, R.W., Chescheir, G.M., Jones, J., 2014. DRAINMOD–DSSAT model for simulating hydrology, soil carbon and nitrogen dynamics, and crop growth for drained crop land. Agric. Water Manag 137, 30–45.
Nosetto, M.D., Jobbágy, E.G., Brizuela, A.B., Jackson, R.B., 2012. The hydrologic consequences of land cover change in central Argentina. Agric. Ecosyst. Environ. 154, 2–11.
Nosetto, M.D., Jobbágy, E.G., Jackson, R.B., Sznaider, G.A., 2009. Reciprocal influence of crops and shallow ground water in sandy landscapes of the Inland Pampas. Field Crop. Res. 113 (2), 138–148.
Nosetto, M.D., Paez, R.A., Ballesteros, S.I., Jobbágy, E.G., 2015. Higher water-table levels and flooding risk under grain vs. livestock production systems in the subhumid plains of the Pampas. Agric. Ecosyst. Environ. 206, 60–70.
Paruelo, J.M., Guerschman, J.P., Verón, S.R., 2005. Expansión agrícola y cambios en el uso del suelo. Ciencia Hoy 87, 14–23.
Podestá, G.P., Messina, C.D., Grondona, M.O., Magrin, G.O., 1999. Associations between grain crop yields in Central-Eastern Argentina and El Niño-Southern oscillation. J. Appl. Meteorol. 38 (10), 1488–1498.
Portela, S.I., Andriulo, A.E., Jobbágy, E.G., Sasal, M.C., 2009. Water and nitrate exchange between cultivated ecosystems and groundwater in the Rolling Pampas. Agric. Ecosyst. Environ. 134, 277–286.
Railsback, S.F., Grimm, V., 2012. Agent-Based and Individual-Based Modeling: A Practical Introduction. Princeton University Press, Princeton, USA.
Reeves, H.W., Zellner, M.L., 2010. Linking MODFLOW with an agent-based land-use model to support decision making. Ground Water 48 (5), 649–660.
Refsgaard, J.C., Storm, B., 1995. Mike SHE. In: Singh, V.P. (Ed.), Computer Models of Watershed Hydrology. Water Resources Publications, pp. 809–846.
Refsgaard, J.C., Storm, B., Clausen, T., 2010. Système Hydrologique Européen (SHE): review and perspectives after 30 years development in distributed physically-based hydrological modelling. Nord. Hydrol 41 (5), 355–377.
Rosegrant, M.W., Ringler, C., Zhu, T., 2009. Water for agriculture: maintaining food security under growing scarcity. Annu. Rev. Environ. Resour. 34 (1), 205–222.
Rusticucci, M., Penalba, O., 2000. Interdecadal changes in the precipitation seasonal cycle over Southern South America and their relationshio with surface temperature. Clim. Res. 16, 1–15.
Satorre, E.H., Benech Arnold, R.L., Slafer, G.A., de la Fuente, E.B., Miralles, D.J., Otegui, M.E., Savin, R., 2003. Producción de granos. Bases funcionales para su manejo. Editorial Facultad de Agronomía, Buenos Aires, Argentina.
Schwartz, R.C., Baumhardt, R.L., Evett, S.R., 2010. Tillage effects on soil water redistribution and bare soil evaporation throughout a season. Soil Tillage Res. 110 (2), 221–229.
Sheaffer, C.C., Tanner, C.B., Kirkham, M.B., 1988. Alfalfa water relations and Irrigation. In: Hanson, A.A. (Ed.), Alfalfa and Alfalfa Improvement. Agronomy Monograph No. 29. ASA- CSSA-SSSA, Madison, USA, pp. 373–409.
Šimůnek, J., van Genuchten, M.T., Šejna, M., 2005. The HYDRUS-1D Software Package for Simulating the Movement of Water, Heat, and Multiple Solutes in Variably Saturated Media, Version 3.0, HYDRUS Software Series 1. Department of Environmental Sciences, University of California Riverside: Riverside, USA.
Sinclair, T.R., Salado-Navarro, L.R., Salas, G., Purcell, L.C., 2007. Soybean yields and soil water status in Argentina: simulation analysis. Agric. Syst. 94 (2), 471–477.
Skaggs, R.W., 1978. A Water Management Model for Shallow Water Table Soils. Technical Report No. 134. Water Resources Research Institute, University of North Carolina, Raleigh, NC, USA.
Viglizzo, E.F., Frank, F.C., Carreño, L.V., Jobbágy, E.G., Pereyra, H., Clatt, J., Pincén, D., Ricard, M.F., 2011. Ecological and environmental footprint of 50 years of agricultural expansion in Argentina. Global Change Biol. 17 (2), 959–973.
Viglizzo, E.F., Jobbágy, E.G., Frank, F.C., Aragón, R., De Oro, L., Salvador, V., 2009. The dynamics of cultivation and floods in arable lands of Central Argentina. Hydrol. Earth Syst. Sci. 13, 491–502.
Voinov, A., Jenni, K., Gray, S., Kolagani, N., Glynn, P.D., Bommel, P., Prell, C., Zellner, M., Paolisso, M., Jordan, R., Sterling, E., Schmitt Olabisi, L., Giabbanelli, P. J., Sun, Z., Le Page, C., Elsawah, S., BenDor, T.K., Hubacek, K., Laursen, B.K., Jetter, A., Basco-Carrera, L., Singer, A., Young, L., Brunacini, J., Smajgl, A., 2018. Tools and methods in participatory modeling: selecting the right tool for the job. Environ. Model. Software 109, 232–255.
Wada, Y., van Beek, L.P.H., van Kempen, C.M., Reckman, J.W.T.M., Vasak, S., Bierkens, M.F.P., 2010. Global depletion of groundwater resources. Geophys. Res. Lett. 37 (20).
Zellner, M.L., 2007. Generating policies for sustainable water use in complex scenarios: an integrated land-use and water-use model of monroe county, Michigan. Environ. Plann. Plann. Des. 34 (4), 664–686.
Zellner, M.L., 2008. Embracing complexity and uncertainty: the potential of agent-based modeling for environmental planning and policy. Plann. Theor. Pract. 9, 437–457.
Zellner, M.L., Lyons, L., Milz, D., Shelley, J., Hoch, C., Massey, D., Radinsky, J., (in press). Participatory complex systems modeling for environmental planning: opportunities and barriers to learning and policy innovation, In: Porter, W., Zhao, J., Scmitt Olabisi, L., McNall, M. (Eds.), Innovations in Collaborative Modeling. Michigan State University Press: East Lansing, USA.
Zellner, M.L., Lyons, L.B., Hoch, C.J., Weizeorick, J., Kunda, C., Milz, D.C., 2012. Modeling, learning, and planning together: an application of participatory agent-based modeling to environmental planning. URISA J. 24 (1), 77–92.
Zellner, M.L., Reeves, H.W., 2010. Integrating land-use and groundwater modeling: opportunities, challenges and implications for policy analysis. Int. J. Oper. Quant. Manag. Spec. Iss. Decis. Mak. Compl. Syst. 16 (4), 389–414.